

## Full length article

## Loading optimization of mixed-type containers for double-stack trains in multi-hub logistics

Zhongbin Zhao<sup>a</sup>, Jihong Chen<sup>b,c,\*</sup>, Mengru Shen<sup>a, \*\*</sup>, Zheng Wan<sup>d</sup>, Hao Wang<sup>e</sup>, Linlan Yu<sup>f</sup><sup>a</sup> School of Traffic and Transportation, Beijing Jiaotong University, Beijing, China<sup>b</sup> College of Management, Shenzhen University, Shenzhen, Guangdong, China<sup>c</sup> Center for Marine Development, Macau University of Science and Technology, Macau<sup>d</sup> College of Transport and Communications, Shanghai Maritime University, Shanghai, China<sup>e</sup> Ocean College, Zhejiang University, Zhoushan, Zhejiang, China<sup>f</sup> School of Navigation, Wuhan University of Technology, Wuhan, Hubei, China

## ARTICLE INFO

## Keywords:

Double-stack container train  
Loading plan  
Hybrid GA-SA  
Intermodal transport  
Multiple hubs

## ABSTRACT

Electrified double-stack container trains (DSTs) play a crucial role in modern logistics by offering increased capacity per trip, reduced rail car usage, lower transportation costs, and fewer emissions. However, optimizing container loading for DSTs is challenging due to constraints such as height limits, center of gravity balance, and other operational requirements. This paper introduces a mixed-integer programming (MIP) model aimed at maximizing transportation efficiency in multi-hub logistics networks, which include intermodal terminals and freight stations. The model supports mixed loading of containers of varying lengths (20/40/48 feet), heights (standard/high cube), load statuses (empty/loaded), and types (regular/foldable), originating from and destined for different locations. Additionally, it incorporates the combination of double-stack container well cars with other rail car types, increasing flexibility in rail car organization and accelerating DST departure times. To solve the complex loading problem, a hybrid genetic algorithm combined with simulated annealing (hybrid GA-SA) is developed. The hybrid GA-SA demonstrates strong performance in numerical case studies across different scales, significantly reducing the number of rail cars needed for large-scale logistics operations while achieving optimal loading configurations. Sensitivity analysis highlights key factors influencing overall transportation benefits. This study offers practical insights for enhancing the operational efficiency and profitability of DSTs and improving container hub throughput within modern logistics networks.

## 1. Introduction

## 1.1. Background

Transhipment operations at intermodal terminal hubs play a pivotal role in container transportation logistics. Traditionally, many terminals rely on trucks to collect and distribute containers, making the optimization of external truck scheduling essential [4]. However, relying heavily on trucks and roadways for container transfers presents several critical challenges: high transportation costs, increased pollution emissions, excessive vehicular energy consumption, and elevated congestion risks. These issues, as highlighted by Chen et al. [2] and Tao et al. [22], exacerbate energy and emissions inefficiencies in container terminals [8,20], ultimately diminishing port competitiveness under rising

environmental pressures [13]. Among them, the port environmental problems are getting increasing attention [17,19].

To address these challenges, a shift from road transport to more sustainable alternatives, such as intermodal transport, is an effective strategy [7,27]. Integrating multiple transportation modes—such as railroads, highways, and waterways—not only reduces transportation costs but also enhances energy efficiency and sustainability. Compared to trucks, container trains are able to move larger volumes of containers in a single trip, alleviating port congestion and reducing disruptions along major transportation routes [11]. In response to increasing demand from larger vessels and growing environmental concerns, terminal operators focus more on rail transport due to the limited availability of gate times and worsening road congestion [18].

In China, the proportion of rail-water intermodal container volume

\* Corresponding author.

\*\* Corresponding author.

E-mail addresses: cxjh2004@163.com (J. Chen), mrschen@bjtu.edu.cn (M. Shen).

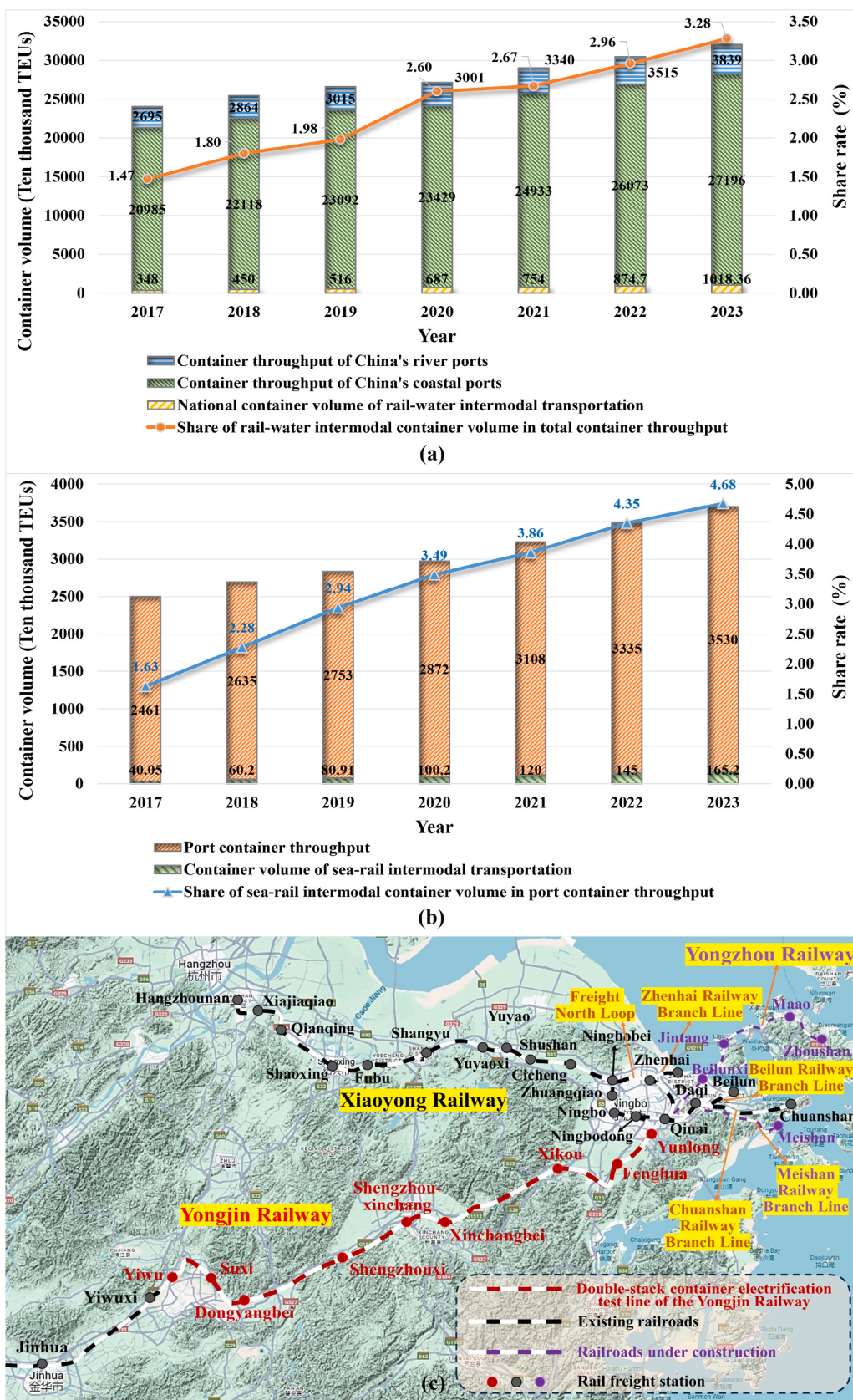


Fig. 1. Overview of rail-water intermodal transportation in China and Ningbo-Zhoushan Port).

Source: (i). Statistical Bulletin on Transportation Sector Development (2017-2023) (ii). Ningbo Zhoushan Port Company Limited (2017-2023)

**Table 1**

Comparison of optimization models for double-stack container trains.

NO.	Literature	Optimization targets	Solution approach	Highlights/gaps
1	[23]	(1) Max. operation profit. (2) Min. total container tardiness.	(1) Problem linearization. (2) Lexicographic optimization. (3) Heuristic algorithm. (4) CPLEX.	(1) Come up with an exact solution method combining lexicographic optimization and the heuristics. (2) The model can reduce the cost of container transportation by about 3 %.
2	[12]	(1) Max. the well car utilization.	(1) Problem linearization. (2) GAMS & CPLEX.	(1) The model enables to develop an optimal loading plan for a DST in a realistic scenario.
3	[9]	(1) Max. TEUs loaded onto the trains. (2) Min. the number of well cars used.	(1) Lagrange relaxation. (2) Genetic algorithm.	(1) The Lagrangian relaxation solution proposed can significantly reduce the computation time.
4	[14]	(1) Min. container cranes' handling time. (2) Max. total TEUs loaded on the train.	(1) Container retrieval heuristic. (2) Container relocation heuristic. (3) Wagon assignment heuristic. (4) Simulated annealing.	(1) This solution reduces crane handling time by 11.79 % compared to the conventional strategy.
5	[10]	(1) Min. the cost of containers left on the ground & railcar cost.	(1) Java and Python programing. (2) CPLEX.	(1) The optimal scheme can be solved within a reasonable running time. (2) Ignore the center of gravity constraint and the matching rule may lead to an infeasible loading plan.
6	[33]	(1) Improve the operational efficiency of the rail-water intermodal terminal.	(1) Design an automatic guided vehicle with a handling function and a new wagon for double-stack containers. (2) Propose a double-stack container yard for container terminals and freight stations.	(1) The synchronous handling scheme for double-stack container trains has significant advantages in reducing container handling time and costs. (2) It reduces the complexity of the loading plans and the organization difficulties of different containers.
7	This paper	(1) Max. the train's benefits on both the outbound and return trips (full round trip).	(1) Analysis of loading modes and technical principles (2) CPLEX for small scale cases.	(1) Investigate the mixed loading of containers with different lengths (20/40/48-ft), heights (high/

**Table 1 (continued)**

NO.	Literature	Optimization targets	Solution approach	Highlights/gaps
				(3) Heuristic algorithms for large scale loading tasks. (4) A hybrid GA-SA designed and programmed in MATLAB.  (3) Mix double-stack container well cars with other types of rail cars. (4) Handle containers at multiple freight stations and terminals (multiple O-Ds).

remains small relative to total container throughput and has shown only modest growth in recent years (see Fig. 1a). For example, Ningbo-Zhoushan Port has considerable potential to expand its containerized sea-rail intermodal business (Fig. 1b). To bridge this gap, and with support from China's Ministry of Transport, the electrified double-stack container pilot line on the Yongjin Railway—connecting Ningbo Yunlong Station to Jinhua Yiwu Station—began operations on December 31, 2023 (Fig. 1c). This initiative is expected to significantly enhance the container collection and distribution capacity of Ningbo-Zhoushan Port, serving as a model project for nationwide adoption. In this context, optimizing the loading plan for electrified double-stack container trains (DSTs) is crucial for improving transport efficiency and terminal transhipment operations.

The loading operations of DSTs present four key challenges: (i) how to allocate different container types to appropriate positions on the double-stack container well cars; (ii) how to determine the optimal loading configuration for each container; (iii) how to minimize the number of well cars required for a given loading task; and (iv) how to maximize transportation benefits when combining well cars with other rail car types. To address these problems, this study proposes a two-part approach. **First**, a systematic analysis of feasible and impractical loading configurations for DSTs is conducted, along with a review of the underlying loading principles. **Second**, a mixed-integer programming (MIP) model is developed and solved using a hybrid genetic algorithm and simulated annealing approach (hybrid GA-SA).

## 1.2. Literature review

### 1.2.1. Loading container trains at the rail-water intermodal terminal

Optimizing container transshipment operations at rail-water intermodal terminals has become a serious challenge for both port and railway operators. It is important to minimize operating costs while ensuring high transshipment efficiency at container terminals [24]. For this reason, researchers have argued that integrated scheduling optimization of multiple equipments in the container terminal helps to achieve efficient handling and transshipment [21,31]. While in the resource allocation for intermodal transport operations, train loading planners need to consider a number of complex factors, including minimizing handling costs, turnaround times and total transportation expenses, as well as allocating containers to specific locations on the train [5]. In order to minimize the times of turning and moving containers in the yard, as well as to reduce the total distance of handling equipment between yards and trains, Siri et al. [16] presented a train loading planning model for a water-rail intermodal container terminal,

which aims to assign containers to the right locations. Yan et al. (2020) also investigated the optimization problem of container transshipment at an intermodal terminal, including train schedule templates and container transshipment planning, which aims to load more containers while reducing the container dwell time at the port [26]. Gharehgozli et al. [3] developed a MIP model for scheduling the handling and unloading of trains by gantry cranes and straddle carriers, with the objective to minimize the total train delay.

### 1.2.2. Transshipment patterns at the container terminal

Incoming containers, after being unloaded from ships, can be loaded directly onto trains (direct transshipment mode), or stored temporarily in yards (indirect transshipment mode). With limited equipment resources and increasing cargo throughput at terminals, the direct transshipment mode can help to improve the operational efficiency, which requires fully coordinated use of various resources while synchronizing the train schedule with the ship's plan [25]. In this respect, Yu et al. [28] examined the operation flow of an automated rail-water container terminal under the direct train-to-ship operation mode and developed a bidirectional scheduling model with the objective of minimizing the total handling time. In practice, to develop a transshipment program between ships and trains, it is necessary to simultaneously determine the train schedule and the container transshipment schedule between ships, yards, and trains. It cannot be ignored that the urgency for containers to be delivered to the shipper/loaded on the liner determines the transshipment mode in which they are selected. This urgency can be indicated by the days before the deadline (DBD). For import containers, the DBD is the number of days between the time of berthing of the container liner and the moment of scheduled delivery requested by the consignee of the bill of lading. For export containers, the DBD is the number of days between the arrival of the DST at the port and the planned loading moment requested by the consignor of the bill of lading.

### 1.2.3. Loading problems of the double-stack container train

Compared to conventional single-stack container trains (SSTs), the deployment of DSTs can increase economies of scale and reduce congestion at ports. For this reason, many countries (including India, the United States, Canada, China and Australia) are constructing new railroads or upgrading existing infrastructure to meet the transportation thresholds required for DST operations [23]. Table 1 compares the relevant publications on loading optimization of DSTs. Considering different weights and heights of containers, Upadhyay et al. [23] developed a DST loading model for profit maximization and delay minimization and subsequently solved it using CPLEX. Ng and Talley [12], on the other hand, proposed a linearized processing optimization model for DST loading and proved that the model can find the optimal loading scheme in real business scenarios. Lin et al. [9] introduced a Lagrangian relaxation method to reduce the time for developing the loading plan of for DSTs. Besides, Rathi & Upadhyay [14] designed a hybrid heuristic method for reducing crane operation time in handling DSTs. The model formulated by Mantovani et al. [10] could also find the optimal DST loading plan in a reasonable time. In addition, Zhao et al. [33] provided a novel synchronized DST handling scheme and demonstrate that it offers obvious advantages in reducing container stevedoring time and operating cost compared to the traditional handling process. In addition, Zhao et al. [32] also employed the DST to transport containers in a collaborative container logistics system between dry ports and water ports.

### 1.3. Research comments and gaps

In summary, research on transshipment optimization at container terminals typically focuses on enhancing efficiency, lowering operational costs, and moving toward sustainable development. In the context of water-rail intermodal transport, researchers have aimed to coordinate resources and optimize handling plans to expedite terminal

transshipment. The use of DSTs is recognized for its ability to improve transportation efficiency and economies of scale. As a result, much of the research in this area focuses on developing loading models with various optimization objectives; as shown in Table 1.

However, there are notable limitations in existing studies. For instance, while mixed loading of 20- and 40-foot containers is commonly addressed, few studies differentiate between general containers (GCs) and high containers (HCs), let alone distinguish between empty and loaded containers. Additionally, foldable containers are rarely considered in these models. Most previous studies also focus on DSTs powered by internal combustion locomotives (such as in the US and India) and do not consider the operational constraints of electrified trains, as seen in China. Furthermore, these articles tend to examine DSTs consisting solely of well cars, neglecting the potential for mixed formations with other rail car types. Finally, the assumption that trains only operate on single one-way trips between an origin terminal and an inland destination fails to consider more complex scenarios involving multiple origin-destination pairs and round-trip shipments. Such assumptions do not fully correspond to realistic rail-water intermodal scenarios.

The optimal loading approach for electrified DSTs proposed in this paper addresses these gaps and offers several key highlights from the following six aspects.

- (1) This paper investigates the mixed loading of 20/40-ft GCs and HCs, both empty and loaded, while also incorporating 40/48-ft foldable containers in the analysis.
- (2) For the first time, the transport mission is implemented on the electrified double-stack container rail line of the Yongjin Railway in China, connecting Ningbo Yunlong Station to Jinhua Yiwu Station.
- (3) The approach enhances the flexibility of train formation by allowing DST well cars to be mixed with other types of rail cars, which accelerates the departure time.
- (4) The trains are designed to handle containers at multiple railroad freight stations and terminal hubs, involving multiple O-D pairs rather than just a single origin-destination pair.
- (5) The total transportation benefits of both outbound and return trips are taken into consideration.
- (6) A hybrid GA-SA method is proposed to optimize the DST loading process, and its reliability and superiority are demonstrated.

The remainder of the paper will be organized as follows. Section 2 will illustrate the feasible and impractical loading modes of DSTs, along with the loading principles that need to be followed. Section 3 constructs a MIP model to maximize the DST transportation benefits. After that, Section 4 will solve an example and discuss the results. While Section 5 summarizes the main work of the article and suggests further research assignments.

## 2. Problem description

### 2.1. Loading forms of double-stack container trains

The study considers three container lengths (20-ft, 40-ft, and 48-ft) in eleven different forms [15]. These include 20-ft loaded and empty containers (comprising both 20-ft GCs and 20-ft HCs), 40-ft loaded and empty containers (also including 40-ft GCs and 40-ft HCs), 40-ft empty foldable container units (40-ft EFC units), as well as 48-ft loaded foldable containers (48-ft LFC units) and empty foldable container units (48-ft EFC units). There exist 20 feasible loading modes for these different containers on the double-stack container well car, as shown in Fig. 2. Modes 21 and 22 are not considered because the containers are loaded on flat cars/wagons instead of well cars. Fig. 3, on the other hand, illustrates 46 theoretically infeasible loading modes. Notably, the height of every four 40-ft empty foldable containers approximately equals the height of an ordinary 40-ft container [6,29,30]. Figs. 2 and 7 also

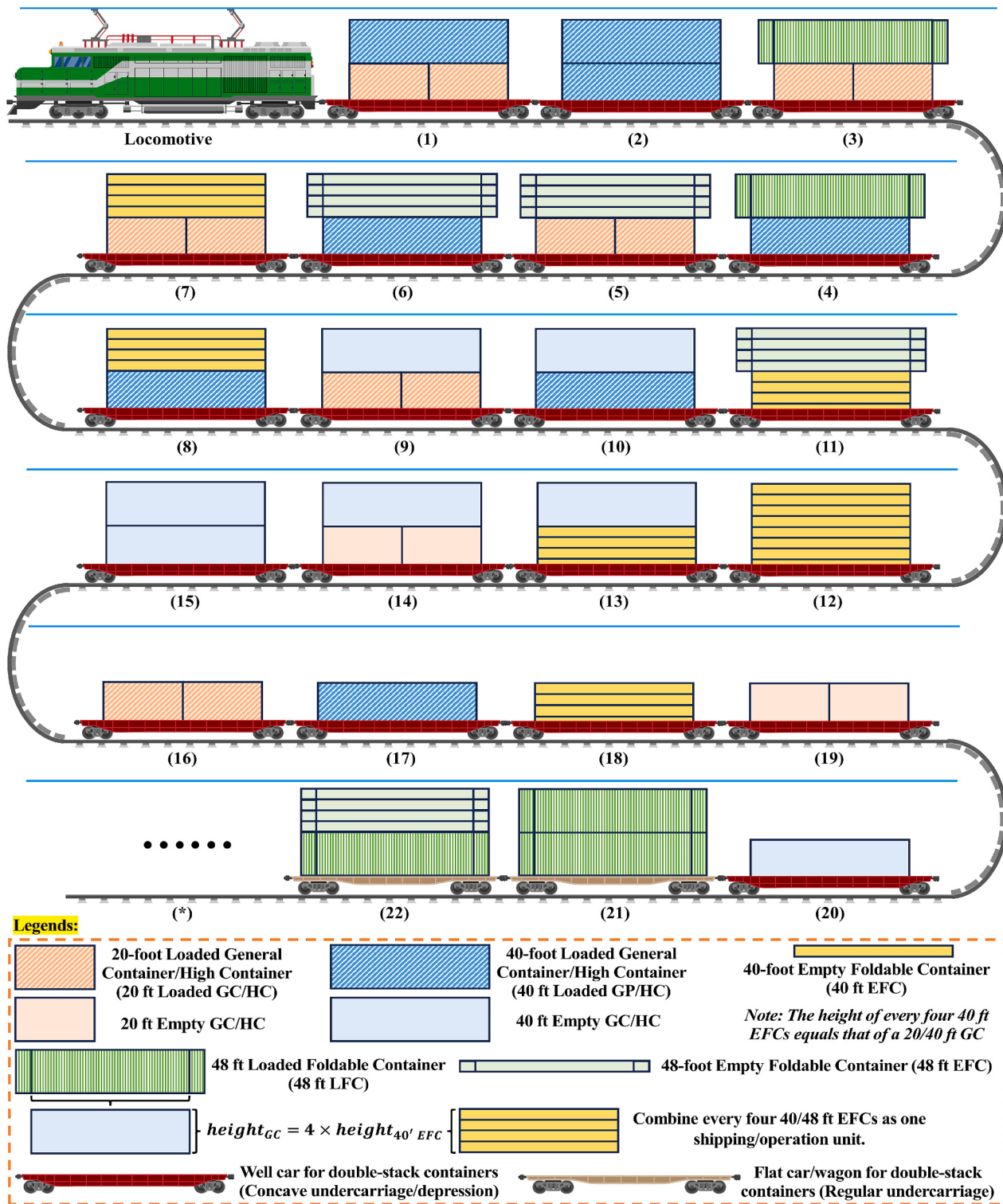


Fig. 2. Feasible loading patterns for double-stack container well cars.

compare the characteristics of the double-stack container well car and the double-stack container flat car. The rest of this paper will be based on the former only.

In the matlab program, we use a matrix to represent the loading pattern of double-stack well cars; see Fig. 4. The number of rows is different for each loading mode and they represent how many containers are in that pattern. In each row, the first number represents the layer number (1/2); the second number denotes the horizontal number (1/2); the third number is the container lengths (20 ft-1, 40 ft-2, 48 ft-3); the

fourth number stands for the container loads (empty -0, loaded-1, EFC unit-2). For example, in the first feasible loading mode, there are three containers (hence three rows of this matrix), including two 20-ft GCs in the lower layer and one 40-ft GC in the upper layer. each container corresponds to a layer number, horizontal number, length, and load indicated by a corresponding digit.

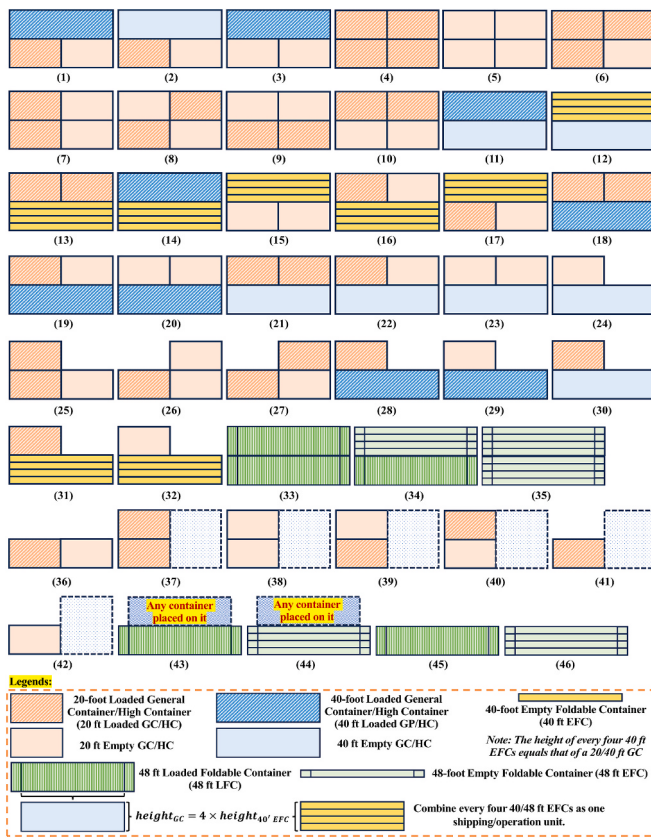


Fig. 3. Impractical loading patterns for double-stack container well cars.

## 2.2. Principles of loading operations

In operations, the loading of DSTs and well cars is subject to the following rules.

- (1) In Fig. 5, DST may stop at several different terminal hubs in the port area for loading of containers/cargoes, which are subsequently transported to several different inland rail freight station hubs for unloading; similarly, DST may stop at several different inland rail freight station hubs for loading of containers/cargoes, which are thereafter delivered to several different terminal hubs for discharging.
- (2) DST is not responsible for transportation of containers/cargoes among hubs of the same type (among railroad freight stations or among terminals).
- (3) Containers and cargoes destined for the same hub need to be organized in successive rail cars.
- (4) Containers and cargoes destined for earlier stops are organized at the rear of the DST and containers/cargo destined for later stops are arranged at the front of the DST according to the order of the DST stops.
- (5) Containers that have been stored at the port longer are prioritized for loading onto the train, while newly arrived containers are loaded afterward, giving precedence to older containers over newer ones.
- (6) Double-stack container well cars must be positioned at the front of other types of rail cars to reduce aerodynamic resistance, as shown in Fig. 6.
- (7) Well cars indexed as  $p \in \{16, 17, 18, 19, 20\}$  should be arranged behind other well cars for the same reason of reducing aerodynamic drag.
- (8) Each well car can either carry 2 20-ft containers simultaneously or none, ensuring consistent loading.
- (9) When carrying two 20-ft containers, the weight difference between them must not exceed the specified limit to maintain balance.
- (10) If two 20-ft containers are loaded on a double-stack well car, they must be placed on the lower deck, not the upper one.
- (11) Additionally, when two 20-ft containers are loaded on the same well car, the height of the two containers shall be the same, i.e., they shall either be HCs or GCs.

```

51 %% Define the loading modes:
52 % 1-layer number; 2-horizontal number;
53 % 3-lengths(20ft-1, 40ft-2, 48ft-3);
54 % 4-loads(empty=0, loaded=1, EFC unit=2)
55 para_load_mode=[];
56 para_load_mode{1}=[1 1 1 1
57     1 2 1 1
58     2 1 2 1];
59 para_load_mode{2}=[1 1 2 1
60     2 1 2 1];
61 para_load_mode{3}=[1 1 1 1
62     1 2 1 1
63     2 1 3 1];
64 para_load_mode{4}=[1 1 2 1
65     2 1 3 1];
66 para_load_mode{5}=[1 1 1 1
67     1 2 1 1
68     2 1 3 2];
69 para_load_mode{6}=[1 1 2 1
70     2 1 3 2];
71 para_load_mode{7}=[1 1 1 1
72     1 2 1 1
73     2 1 2 2];
74 para_load_mode{8}=[1 1 2 1
75     2 1 2 2];
76 para_load_mode{9}=[1 1 1 1
77     1 2 1 1
78     2 1 2 0];
79 para_load_mode{10}=[1 1 2 1
80     2 1 2 0];
81 para_load_mode{11}=[1 1 2 2
82     2 1 3 2];
83 para_load_mode{12}=[1 1 2 2
84     2 1 2 2];
85 para_load_mode{13}=[1 1 2 2
86     2 1 2 0];
87 para_load_mode{14}=[1 1 1 0
88     1 2 1 0
89     2 1 2 0];
90 para_load_mode{15}=[1 1 2 0
91     2 1 2 0];
92 para_load_mode{16}=[1 1 1 1
93     1 2 1 1];
94 para_load_mode{17}=[1 1 2 1];
95 para_load_mode{18}=[1 1 2 2
96     2 1 2 2
97     3 1 2 2
98     4 1 2 2];
99 para_load_mode{19}=[1 1 1 0
100    1 2 1 0];
101 para_load_mode{20}=[1 1 2 0];

```

Fig. 4. Matlab program of the loading modes.

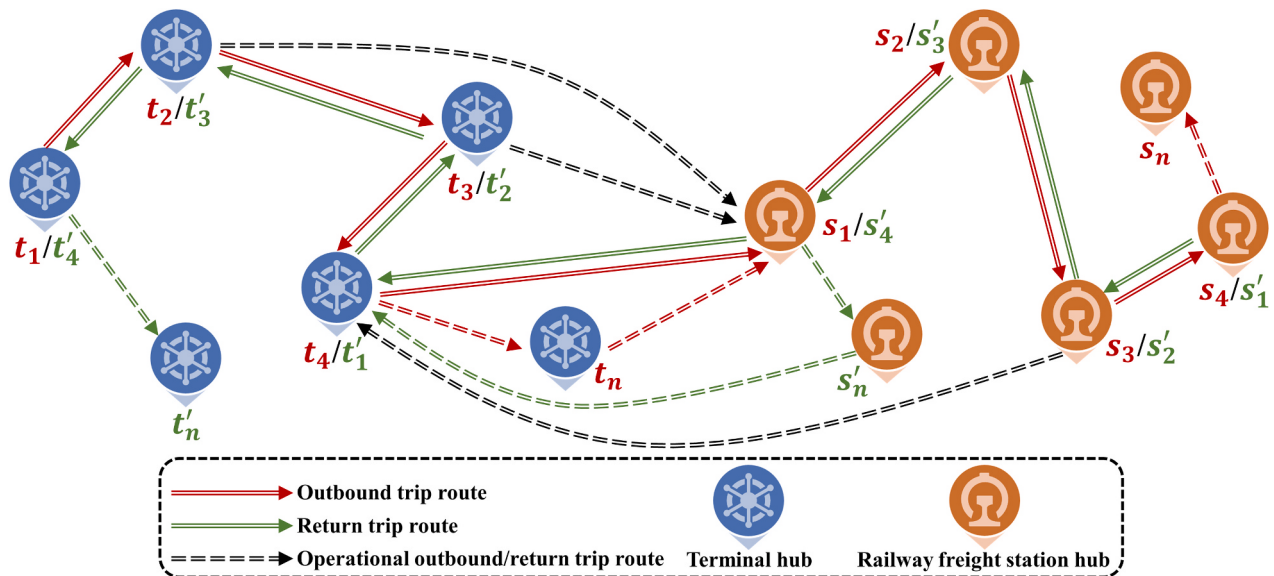


Fig. 5. Rail transportation between different types of hubs.

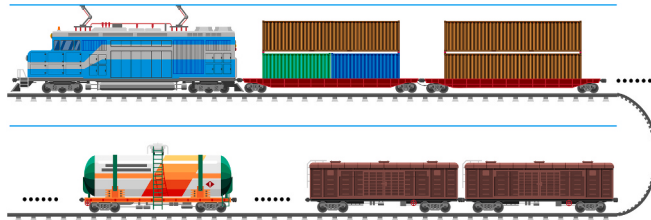


Fig. 6. Mixed grouping of multi types of rail cars.

- (12) The center of gravity of the entire well car, after accounting for its tare weight, height, and the combined gross weight and height of the containers, must not exceed the specified limit.
- (13) The height from the top of the containers loaded on each well car to the overhead contact wire must remain within the prescribed limit (see Fig. 7).
- (14) The total weight of the containers carried by a well car must not exceed its maximum load capacity.
- (15) A 40-ft container can be placed on either the upper or lower deck of the well car; however, the total weight of the containers on the upper deck must not surpass that of those on the lower deck.
- (16) For ease of modeling, each set of double-stack container rail cars is composed of a single well car, and the containers loaded on each well car must be destined for the same destination.

### 2.3. Loading task flow

Based on the feasible loading patterns and the above rules, the loading operation of a DST can be abstracted into five stages. The following Section 3 will implement this process in a mathematical way and the MIP model.

- (1) Assigning 11 types of containers with different lengths (20 ft, 40 ft, 48 ft) and loads (empty, loaded, EFC unit) to suitable locations on the double-stack container well car.
- (2) Determining the loading mode to which each container ultimately belongs on the well car.
- (3) Judging the feasibility of these loading alternatives, i.e., whether they satisfy hard constraints including, but not limited to, load constraints, center of gravity height constraints, height limitations of the tops of the containers carried on the well car from the

contact line, origin & destination requirements, weight differences between upper and lower containers, quantity constraints of the various types of rail cars, and mixed grouping sequences.

- (4) Minimizing the number of well cars required for a given number of containers of each type in a loading task.
- (5) Solving for the loading scheme that maximizes the operational benefits of mixing well cars with other types of rail cars.

## 3. Model formulation

### 3.1. Assumptions

This section establishes a MIP model to maximize the round-trip transportation benefits of the DST. The following assumptions are made.

- (1) Given that the Yongjin Railway double-stack high container pilot line is electrified, the clearance between the upper container and the overhead contact wire is limited. Therefore, only double-stack well cars with depressed centers are used in this study, while flat cars/wagons are excluded; see Fig. 6(a) and 6(b).
- (2) As detailed in Section 2.1, the loading process incorporates eleven types of containers, including 20-ft empty/loaded GCs and HCs, 40-ft empty/loaded GCs and HCs, 40-ft EFC units, 48-ft LFCs and EFC units. Notably, 40-ft LFCs are regarded as 40-ft GCs.
- (3) There are 20 feasible loading forms for double-stack container well cars, as shown in Fig. 2.
- (4) The 20-ft empty/loaded GCs and HCs can only be placed in positions (1) and (2) of the well car. The 40-ft empty/loaded GCs and HCs as well as 40-ft EFC units can only occupy positions (3) and (4), while the 48-ft LFC units and EFC units are limited to position (4).
- (5) In mixed formations, three common railcar types are considered: double-stack container well cars, general-purpose shed cars, and rail tank cars, as illustrated in Fig. 5. Open cars, primarily used for coal transport, are excluded from the model as they typically operate on heavy-haul railways.
- (6) The intermodal train carries a set of containers (charged by the type and quantity, grouped into 11 categories), general cargo (charged by the number of shed cars), and liquid bulk cargo (charged by the number of tank cars).
- (7) The intermodal transportation system comprises T terminal hubs and S rail freight hubs.

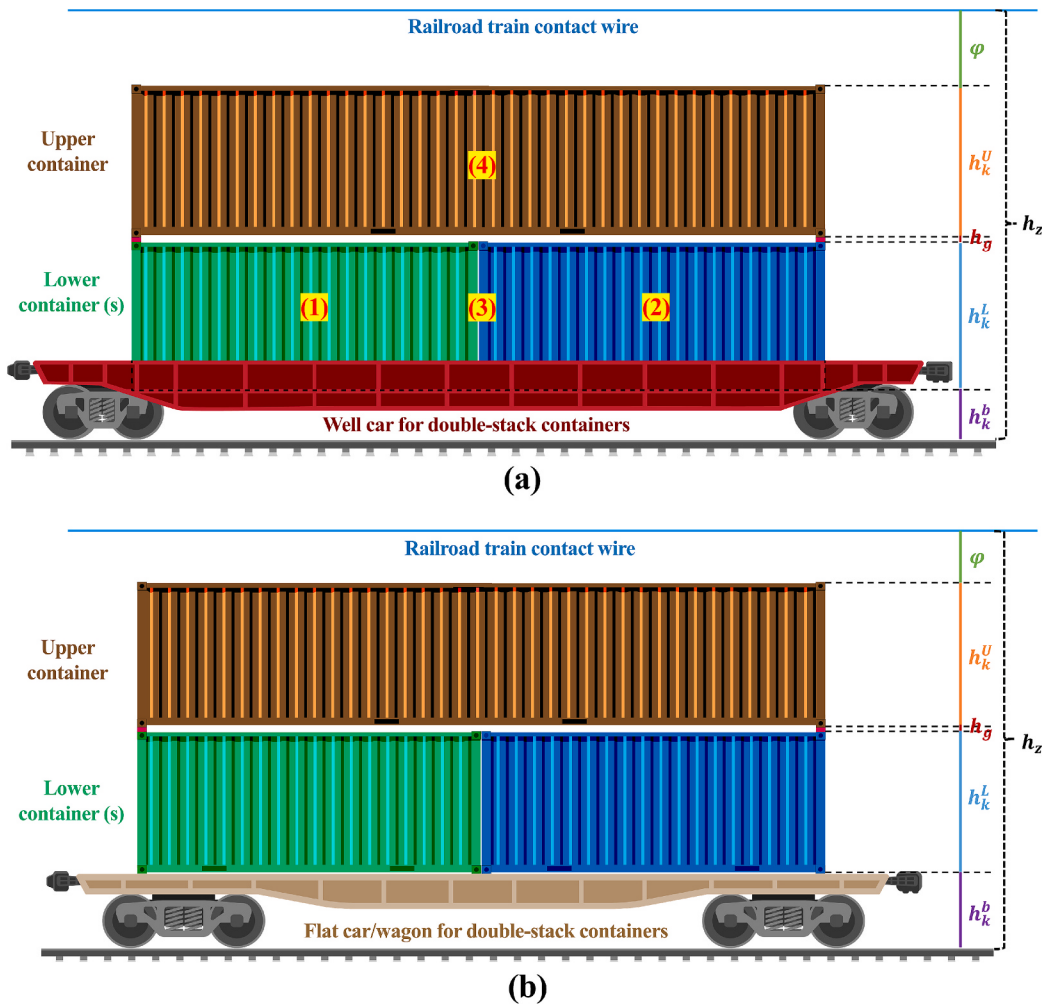


Fig. 7. Comparison of the well car and flat car for double-stack containers.

**Table 2**  
Summary of indexes and sets.

Indices	Description
$c \in C_j$	Container index
$i \in I = \{1, 2, 3\}$	Rail car type index
$j \in J = \{20, 40, 48\}$	Container type index
$p \in P = \{1, 2, \dots, 20\}$	Feasible loading modes for double-stack containers
$l \in L = \{1, 2, 3, 4\}$	Index of container position on the well car
$t \in T = \{1, 2, \dots, t_n\}$	Type T hub index
$s \in S = \{1, 2, \dots, s_n\}$	Type S hub index
$k \in K = \{1, 2, \dots, k_n\}$	Index of the $k$ th well car counting backwards from the locomotive

- (8) The model does not account for train dwell time at each hub.
- (9) It is assumed that both shed cars and tank cars carry full loads, not partial shipments.

#### 4. Notations

Table 2 summarizes the indexes and sets mentioned in the model. Table 3 describes in detail the connotations of each parameter. And Table 4 sets the five decision variables.

- (1) Citations
- (2) Parameters

**Table 3**  
Parameter summary and description.

Parameters	Description
$w_c^{20}$	Gross weight of a 20-ft loaded/empty container (includes GC/HC), $c \in C_{20}, k \in K$
$w_c^{40}$	Gross weight of a 40-ft loaded/empty container (includes GC/HC) or a 40-ft EFC unit, $c \in C_{40}, k \in K$
$w_c^{48}$	Gross weight of a 48-ft LFC or EFC unit, $c \in C_{48}, k \in K$
$b_i^1$	Base freight 1 for each type of rail car (charged by the number of rail cars), $i \in I$
$b_i^2$	Base freight 2 for each type of rail car (charged by the number of rail cars), $i \in I$
$b_j^1$	Base freight 1 for each type of container (charged by the number of containers), $j \in J$
$b_j^2$	Base freight 2 for each type of container (charged according to container-kilometer), $j \in J$
$u_i$	Usage cost of each type of car, $i \in I$
$d_{ts}^i$	The distance that a container is transported from hub T to hub S, $k \in K, t \in T, s \in S$
$d_{ik}^s$	The travel distance of a $k$ th rail car in type $i$ from hub T to hub S, $i \in I, k \in K, t \in T, s \in S$
$v$	Speed of the train
$L$	Locomotive running cost
$D$	The distance the train travels from the first hub T to the last hub S
$\omega$	Well car load limit
$\varphi$	Height limit of the container top on the well car from the contact wire
$\varepsilon$	Height limit of the vertical center of gravity of the well car

**Table 4**  
Summary and description of decision variables.

Decision variables	Description
$\alpha_{ck}^l$	$\alpha_{ck}^l = 1$ if the 20-ft loaded/empty container (includes GC/HC) is placed at location $l$ on the well car $k$ ; 0 otherwise. $c \in C_{20}$ , $l \in \{1, 2\}$ , $k \in K$
$\beta_{ck}^l$	$\beta_{ck}^l = 1$ if the 40-ft loaded/empty container (includes GC/HC) or a 40-ft EFC unit is placed at location $l$ on the well car $k$ ; 0 otherwise. $c \in C_{40}$ , $l \in \{3, 4\}$ , $k \in K$
$\gamma_{ck}^l$	$\gamma_{ck}^l = 1$ if the 48-ft LFC or EFC unit is placed at location $l$ on the well car $k$ ; 0 otherwise. $c \in C_{48}$ , $l = 4$ , $k \in K$
$x_{ik}^{ts}$	$x_{ik}^{ts} = 1$ if the $k_{th}$ rail car in type $i$ travels from hub T to hub S; 0 otherwise. $i \in I$ , $k \in K$ , $t \in T$ , $s \in S$
$y_k^p$	$y_k^p = 1$ if the loading mode of well car $k$ is $p$ ; 0 otherwise. $k \in K$ , $p \in P$

### (3) Decision variables

#### 4.1. Objective functions and constraints

The transportation revenue generated by double-stack container well cars, calculated based on container classification and quantity, can be expressed as follows.

$$\rho = \sum_{k \in K} \left( \sum_{c \in C_{20}} \left[ (\alpha_{ck}^1 + \alpha_{ck}^2) \left( b_{20}^1 + b_{20}^2 \sum_{t \in T} \sum_{s \in S} d_{cs}^{ts} \right) \right] + \sum_{c \in C_{40}} \left[ (\beta_{ck}^3 + \beta_{ck}^4) \left( b_{40}^1 + b_{40}^2 \sum_{t \in T} \sum_{s \in S} d_{cs}^{ts} \right) \right] + \sum_{c \in C_{48}} \gamma_{ck}^4 \left( b_{48}^1 + b_{48}^2 \sum_{t \in T} \sum_{s \in S} d_{cs}^{ts} \right) \right) \quad (1)$$

The transportation revenue for other types of cargo can be expressed in formula (2).

$$\sigma = \sum_{i \in \{2, 3\}} \left[ \left( b_i^1 + b_i^2 \sum_{k \in K} \sum_{t \in T} \sum_{s \in S} d_{ik}^{ts} \right) \times \sum_{k \in K} \sum_{t \in T} \sum_{s \in S} x_{ik}^{ts} \right] \quad (2)$$

The transportation costs can be represented accordingly.

$$\tau = \sum_{i \in I} \sum_{k \in K} \sum_{t \in T} \sum_{s \in S} (u_i x_{ik}^{ts} + L) \left\lceil \frac{2D}{v} \right\rceil \quad (3)$$

The notation  $\lceil \cdot \rceil$  denotes the ceiling function applied to the value of  $\frac{D}{v}$ , indicating that the usage cost for each type of rail car will be charged on an hourly basis, with any duration less than one hour counted as a full hour. Therefore, the objective function to maximize the transportation benefits is as follows.

$$MaxR \equiv \rho + \sigma - \tau \quad (4)$$

The model is subject to the following constraints.

$$\sum_{p \in P} y_k^p = 1, \forall k \in K \quad (5)$$

$$\sum_{k \in K} \sum_{l \in \{1, 2\}} \alpha_{ck}^l \leq 1, \forall c \in C_{20} \quad (6)$$

$$\sum_{k \in K} \sum_{l \in \{3, 4\}} \beta_{ck}^l \leq 1, \forall c \in C_{40} \quad (7)$$

$$\sum_{k \in K} \sum_{l=4} \gamma_{ck}^l \leq 1, \forall c \in C_{48} \quad (8)$$

$$\left| \sum_{c \in C_{20}} w_c^{20} (\alpha_{ck}^1 - \alpha_{ck}^2) \right| \leq \delta, \forall k \in K \quad (9)$$

$$\sum_{c \in C_{20}} w_c^{20} (\alpha_{ck}^1 - \alpha_{ck}^2) \leq \delta, \forall k \in K \quad (10)$$

$$\sum_{c \in C_{20}} w_c^{20} (\alpha_{ck}^1 - \alpha_{ck}^2) \geq -\delta, \forall k \in K \quad (11)$$

$$\sum_{i \in I} \sum_{t \in T} \sum_{s \in S} x_{ik}^{ts} = 1, \forall k \in K \quad (12)$$

$$\sum_{c \in C_{20}} h_c (\alpha_{ck}^1 - \alpha_{ck}^2) \leq \sum_{p \in \{1, 3, 5, 7, 9, 14\}} (1 - y_k^p), \forall k \in K \quad (13)$$

$$\sum_{c \in C_{20}} h_c (\alpha_{ck}^1 - \alpha_{ck}^2) \geq \sum_{p \in \{1, 3, 5, 7, 9, 14\}} (y_k^p - 1), \forall k \in K \quad (14)$$

$$G_k = \frac{Q_k W_k + (h_k^b + h_k^L/2) W_k^L + (h_k^b + h_k^L + h_g + h_k^U/2) W_k^U}{W_k + W_k^L + W_k^U} \leq \varepsilon, \forall k \in K \quad (15)$$

$$h_k^L = \frac{1}{2} \sum_{c \in C_{20}} \sum_{l \in \{1, 2\}} h_c \alpha_{ck}^l + \sum_{c \in C_{40}} h_c \beta_{ck}^3, \forall k \in K \quad (16)$$

$$h_k^U = \sum_{c \in C_{40}} h_c \beta_{ck}^4 + \sum_{c \in C_{48}} h_c \gamma_{ck}^4, \forall k \in K \quad (17)$$

$$W_k^L = \sum_{c \in C_{20}} \sum_{l \in \{1, 2\}} w_c^{20} \alpha_{ck}^l + \sum_{c \in C_{40}} w_c^{40} \beta_{ck}^3, \forall k \in K \quad (18)$$

$$W_k^U = \sum_{c \in C_{40}} w_c^{40} \beta_{ck}^4 + \sum_{c \in C_{48}} w_c^{48} \gamma_{ck}^4, \forall k \in K \quad (19)$$

$$h_z - (h_k^b + h_g + h_d) - \left( \sum_{c \in C_{20}} \sum_{l \in \{1, 2\}} h_c \alpha_{ck}^l + \sum_{c \in C_{40}} h_c \beta_{ck}^3 \right) - \left( \sum_{c \in C_{40}} h_c \beta_{ck}^4 + \sum_{c \in C_{48}} h_c \gamma_{ck}^4 \right) \leq \varphi, \forall k \in K \quad (20)$$

$$\sum_{c \in C_{20}} \sum_{l \in \{1, 2\}} w_c^{20} \alpha_{ck}^l + \sum_{c \in C_{40}} \sum_{l \in \{3, 4\}} w_c^{40} \beta_{ck}^l + \sum_{c \in C_{48}} w_c^{48} \gamma_{ck}^4 \leq \omega, \forall k \in K \quad (21)$$

$$\sum_{c \in C_{20}} w_c^{20} (\alpha_{ck}^1 + \alpha_{ck}^2) + \sum_{c \in C_{40}} w_c^{40} \beta_{ck}^3 \geq \sum_{c \in C_{40}} w_c^{40} \beta_{ck}^4 + \sum_{c \in C_{48}} w_c^{48} \gamma_{ck}^4, \forall k \in K \quad (22)$$

$$k_{p_1} < k_{p_2}, \forall p_1 \in P_1, \forall p_2 \in P_2 \quad (23)$$

$$k_1 < k_2, \forall k_1 \in K_1, \forall k_2 \in K_2 \quad (24)$$

$$k_1 < k_3, \forall k_1 \in K_1, \forall k_3 \in K_3 \quad (25)$$

$$\sum_{k_1 \in K_1} k_1 + \sum_{k_2 \in K_2} k_2 + \sum_{k_3 \in K_3} k_3 \leq \theta, \forall k_1 \in K_1, \forall k_2 \in K_2, \forall k_3 \in K_3 \quad (26)$$

$$\alpha_{ck}^l \in \{0, 1\}, \forall c \in C_{20}, \forall k \in K, \forall l \in \{1, 2\} \quad (27)$$

$$\beta_{ck}^l \in \{0, 1\}, \forall c \in C_{40}, \forall k \in K, \forall l \in \{3, 4\} \quad (28)$$

$$\gamma_{ck}^l \in \{0, 1\}, \forall c \in C_{48}, \forall k \in K, \forall l \in \{4\} \quad (29)$$

$$x_{ik}^{ts} \in \{0, 1\}, \forall i \in I, \forall k \in K, \forall t \in T, \forall s \in S \quad (30)$$

$$y_k^p \in \{0, 1\}, \forall k \in K, \forall p \in P \quad (31)$$

Constraint (5) establishes that each double-stack container well car can select only one loading mode. Constraints (6) to (8) specify that each container or EFC unit can occupy only one position on each well car. Constraint (9) indicates that when a well car transports two 20-ft containers, the weight difference between them must not exceed a

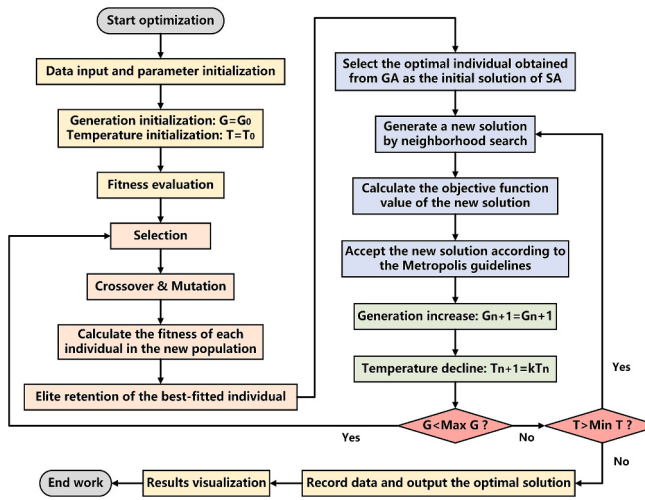


Fig. 8. Flowchart of Hybrid GA-SA.

specified value. This constraint is nonlinear and can be reduced to two linear Constraints (10) ~ (11). Constraint (12) restricts each well car to transport containers or EFC units from one hub T to another hub S. Constraints (13) and (14) require that the heights of the two 20-ft containers on a well car must be consistent, meaning both must either be HCs or GCs.

Constraints (15) to (19) set limits on the center of gravity of the entire car, considering the weight and height of the empty well car as well as the total weight and height of the containers or EFC units.  $Q_k$  denotes the center of gravity height of the empty well car, set at 650 mm, while  $W_k$  represents its weight, which is 22 tons.  $h_k^b$  indicates the height from the well car's loading surface to the track, measured at 290 mm. Additionally,  $h_k^l$  and  $h_k^U$  refer to the heights of the lower and upper containers, respectively. The height of the reinforcing connector is denoted by  $h_g$ .  $W_k^l$  and  $W_k^U$  represent the weights of the lower and upper containers, respectively. In the calculations, the height for both 20/40-ft GCs and 40/48-ft LFCs/EFC units is set at 2591 mm, while the height for both 20/40-ft HCs is 2896 mm.

Furthermore, Constraint (20) mandates that the height from the top of the containers to the contact line must remain within prescribed limits. This constraint can also be understood against Fig. 7. Among this,  $h_z$  represents the height of the railway contact line above ground, measured at 6330 mm. While  $h_g$ , taken as 30 mm, is the height of the reinforcing connector. The sag of the contact wire is denoted by  $h_d$  and is set at 50 mm. And  $h_c$  signifies the height of the container/EFC unit.

In addition, Constraint (21) specifies that the total weight of the containers on each well car must not exceed its load capacity. Furthermore, Constraint (22) requires that the total weight of the upper containers or EFC units must not exceed that of the lower ones. To minimize aerodynamic drag, well cars with loading mode  $p \in \{16, 17, 18, 19, 20\}$  should be positioned behind well cars of other types. If we introduce  $p_1 \in P_1 = \{1, 2, \dots, 15\}$  and  $p_2 \in P_2 = \{16, 17, \dots, 20\}$ , this can be articulated in Constraint (23). All well cars must be placed at the front of other types of rail cars to further reduce aerodynamic resistance. Let  $k_i \in K_i = \{1, 2, \dots, k_i\}$  represent the identifiers for three different types of rail cars, where  $i \in I = \{1, 2, 3\}$ , resulting in Constraints (24) to (25). Constraint (26) specifies that the total number of all types of rail cars must not exceed the maximum allowed for a single train. Finally,

Constraints (27) to (31) define the binary variables.

#### 4.2. Solution approach

DST loading optimization requires the consideration of various constraints, such as load limit, maximum height limit, center of gravity distribution, mixed loading of different container types, and multi-hub handling demands, etc. This problem is essentially an NP-hard problem with multiple local optimal solutions, which is difficult to be solved effectively by simple optimization algorithms, especially when the solution space is very large.

The traditional Genetic Algorithm (GA) is effective for global searches, as it can explore a wide solution space. However, it is prone to getting stuck in local optima. In contrast, the Simulated Annealing algorithm (SA) is better suited for local searches, allowing for fine-tuning within a neighborhood of solutions, though it converges more slowly [1]. To combine the strengths of both methods, a hybrid GA-SA is proposed. In the global search phase, GA identifies a set of promising initial solutions. Then, in the local optimization phase, SA takes the best individuals from GA as initial solutions and further refines them through local search to enhance solution quality. This process is illustrated in Fig. 8 and Algorithm 1.

Hybrid GA-SA can flexibly deal with the diversities in the loading problem because it realizes the complementary advantages of the two algorithms, which can balance the solution quality and computational efficiency in global search and local optimization. More significantly, since the DST loading problem requires both macroscopic planning of loading modes and microscopic optimization of specific loading

**Table 6**  
Summary of experimental parameter values.

Parameters	Value
Speed of the train	$v = 120\text{km}/\text{h}$
Locomotive running cost	$L = 2500\text{CNY}/\text{h}$
The travel distance of the train from the first hub T to the final hub S	$D = 1600\text{km}$
Limit for the difference in weight between two 20-ft containers on the same layer	$\delta = 10\text{ton}$
Well car load limit	$\omega = 78\text{ton}$
Height limit of the container top on the well car from the contact wire	$\varphi = 350\text{mm}$
Height limit of the vertical center of gravity of the well car	$\varepsilon = 2400\text{mm}$
Maximum total number of groupings per train stipulated	$\theta = 60\text{railcars}$
Base freight 1 for 20-ft containers	$440\text{CNY}/\text{unit}$
Base freight 2 for 20-ft containers	$3.185\text{CNY}/\text{unit} \bullet \text{km}$
Base freight 1 for 40-ft containers	$532\text{CNY}/\text{unit}$
Base freight 2 for 40-ft containers	$3.357\text{CNY}/\text{unit} \bullet \text{km}$
Base freight 1 for 48-ft containers	$650\text{CNY}/\text{unit}$
Base freight 2 for 48-ft containers	$3.516\text{CNY}/\text{unit} \bullet \text{km}$
Base freight 1 for shed cars	$768\text{CNY}/\text{railcar}$
Base freight 2 for shed cars	$5.46\text{CNY}/\text{railcar} \bullet \text{km}$
Base freight 1 for tank cars	$930\text{CNY}/\text{railcar}$
Base freight 2 for tank cars	$5.15\text{CNY}/\text{railcar} \bullet \text{km}$
Usage cost of the well car	$100\text{CNY}/\text{railcar} \bullet \text{h}$
Usage cost of the shed car	$150\text{CNY}/\text{railcar} \bullet \text{h}$
Usage cost of the tank car	$180\text{CNY}/\text{railcar} \bullet \text{h}$

Notes: (i) The base freight rate is the same for containers of the same length (20-ft, 40-ft, 48-ft), whether they are loaded or empty, and whether they are GCs or HCs (<https://ec.95306.cn/infoDetail-goodsRate>).  
(ii) Each P70A-type shed car has a cargo capacity of 60 tons (<https://ec.95306.cn/infoDetail-boxcar>).  
(iii) The cargo capacity of each G70A-type tank car is 50 tons (<https://ec.95306.cn/infoDetail-tankcar>).

**Table 5**  
Distance between the hubs.

T1-S1	T1-S2	T1-S3	T2-S1	T2-S2	T2-S3	T3-S1	T3-S2	T3-S3
1200 km	1400 km	1600 km	1100 km	1300 km	1500 km	1000 km	1200 km	1400 km

**Table 7**

Data for 50 containers and EFC units.

Container type (ft)	Loaded or empty container/ unit	Container index	Container height (mm)	Full container weight (ton)	Citation of hub T	Citation of hub S
20	LHC	1	2896	19.88	1	1
20	LHC	2	2896	19.48	1	1
20	LGC	3	2591	21.24	1	2
20	LGC	4	2591	21.74	1	2
20	LHC	5	2896	18.27	1	2
20	LHC	6	2896	19.12	1	2
20	LHC	7	2896	20.86	3	2
20	LHC	8	2896	21.95	3	2
20	LHC	9	2896	17.57	1	3
20	LHC	10	2896	22.27	1	3
20	EGC	11	2591	2.30	1	2
20	EGC	12	2591	2.30	1	2
20	EGC	13	2591	2.30	2	2
20	EGC	14	2591	2.30	2	2
20	EHC	15	2896	2.32	2	1
20	EHC	16	2896	2.32	2	1
20	EGC	17	2591	2.30	2	2
20	EGC	18	2591	2.30	2	2
20	EGC	19	2591	2.30	2	2
20	EGC	20	2591	2.30	2	2
40	LGC	1	2591	24.26	3	1
40	LHC	2	2896	27.78	1	1
40	LHC	3	2896	26.47	1	1
40	LHC	4	2896	25.76	1	1
40	LGC	5	2591	24.44	1	1
40	LGC	6	2591	23.59	1	2
40	LHC	7	2896	26.47	1	2
40	LGC	8	2591	23.45	3	2
40	LGC	9	2591	24.37	1	2
40	LGC	10	2591	22.85	3	1
40	EGC	11	2591	3.75	2	2
40	EGC	12	2591	3.75	1	2
40	EHC	13	2896	3.94	2	2
40	EHC	14	2896	3.94	2	2
40	EHC	15	2896	3.94	1	3
40	EFC unit	16	2591	20.00	2	3
40	EFC unit	17	2591	20.00	3	3
40	EFC unit	18	2591	20.00	3	3
40	EFC unit	19	2591	20.00	3	3
40	EFC unit	20	2591	20.00	3	3
48	LFC	1	2591	19.48	3	1
48	LFC	2	2591	17.76	1	1
48	LFC	3	2591	19.56	3	2
48	LFC	4	2591	18.12	3	2
48	LFC	5	2591	18.72	1	2
48	EFC unit	6	2591	18.00	2	3
48	EFC unit	7	2591	18.00	3	3
48	EFC unit	8	2591	18.00	3	3
48	EFC unit	9	2591	18.00	3	3
48	EFC unit	10	2591	18.00	3	3

Notes: (i) Abbreviations: EGC for Empty General Container, EHC for Empty High Container, LGC for Loaded General Container, LHC for Loaded High Container, LFC for Loaded Foldable Container, and EFC Unit for Empty Foldable Container Unit.

(ii) The tare weight of each 40-ft EFC in a 40-ft EFC unit is 5 tons (<https://container-xchange.cn/blog/flat-rack-0-container/>).

(iii) Each EFC in a 48-ft EFC unit has a tare weight of 4.5 tons (<https://spe.coscoshipping.com/main/digitalsolution-content?model=10982>).

(iv) Tare weight per 20-ft and 40-ft GC is 2.30 tons and 3.75 tons, respectively (<https://container-xchange.cn/blog/container-types-and-dimensions/>).

(v) Tare weight per 20-ft and 40-ft HC is 2.32 tons and 3.94 tons, respectively (<https://container-xchange.cn/blog/high-cube-containers-2/>).

**Table 8**  
General cargo data.

General cargo index	Full shed car weight (ton)	Citation of hub T	Citation of hub S	Shed car k citation
1	60	1	3	1
2	60	1	3	2
3	60	2	1	7
4	60	2	1	8
5	60	2	1	9
6	60	2	1	10
7	60	2	1	11
8	60	2	1	12
9	60	2	2	3
10	60	2	2	4
11	60	2	2	5
12	60	2	2	6
13	60	1	1	13
14	60	1	1	14
15	60	1	1	15

**Table 9**  
Liquid bulk cargo data.

Liquid bulk cargo index	Full tank car weight (ton)	Citation of hub T	Citation of hub S	Tank car k citation
1	50	3	1	9
2	50	3	1	10
3	50	3	2	6
4	50	3	2	7
5	50	3	2	8
6	50	3	3	1
7	50	3	3	2
8	50	3	3	3
9	50	3	3	4
10	50	3	3	5
10	50	3	3	6

**Table 10**  
Best combination of hybrid GA-SA parameters.

Parameter	Abbreviation	Range	Best value
Population size	pop_size	[20, 100]	100
Maximum GA iterations	max_ga_gen	[50, 100]	100
Crossover probability	cross_prob	[0.4, 0.99]	0.9
Mutation probability	mut_prob	[0.01, 0.29]	0.1
Elite retention ratio	elite_rate	[0.05, 0.2]	0.15
Maximum SA iterations	max_sa_gen	[50, 200]	100
Initial temperature	T0	[100, 500]	300
Annealing coefficient	alfa	[0.8, 0.99]	0.95

alignments, hybrid GA-SA is able to take into account both needs, and can flexibly adjust the fitness function and optimization process with the specific characteristics of the problem (e.g., loading rules, train allocations, and the number of containers) to ensure the practicability of the algorithm. Hybrid GA-SA can also flexibly adjust the fitness function and optimization process to ensure the practicality of the algorithm. In this research, the hybrid GA-SA approach follows four main steps.

### (1) Data input and initialization

**Table 11**  
Computational performance of different methods for 50 containers and EFC units.

Approach	Loading task for 50 containers and EFC units			Loading task for 100 containers and EFC units		
	Iterations	Computation time (s)	GAP (%)	Iterations	Computation time (s)	GAP (%)
Hybrid GA-SA	66	38.125	N/A	77	84.265	N/A
SA	68	47.218	-19.26 %	83	98.433	-14.39 %
GA	90	66.086	-42.31 %	89	163.638	-48.51 %
CPLEX	N/A	41.257	-7.59 %	N/A	121.352	-30.56 %

(i) Input container data, cargo data, rail car parameters, and constraints from the Excel file. This includes container information (volume, lengths, heights, loads, weights, shapes, O-Ds and freight rates) and cargo data (quantities, weights, O-Ds and freight rates). Additionally, the input also includes the number of different rail cars, load limits, maximum height, and center of gravity restrictions. (ii) Define 20 loading modes based on container characteristics to arrange containers in each mode. During the calculation, each container will be assigned to a location on the right layer of the well car.

### (2) Global search by GA

(i) Randomly generate an initial population, where each individual represents a potential loading plan. (ii) Evaluate the fitness of each individual in the population. Fitness is determined by the objective function, 'fun\_1', which incorporates both optimization function and constraints. (iii) Select parents based on fitness values by the roulette wheel to generate individuals for the next generation. (iv) Perform crossover between two selected parents to generate offspring, blending characteristics of both parents by randomly selecting crossover points. (v) Introduce diversity by randomly mutating some genes in the offspring, promoting new solution possibilities. (vi) Retain the fittest individuals with elite strategy to prevent deterioration of solutions across generations.

### (3) Local optimization by SA

(i) Use the best individual obtained from the GA process as the initial solution for SA. (ii) Set the initial temperature and define the cooling rate along with the iterations for each temperature. (iii) Generate new solutions within the neighborhood of the current solution and evaluate the objective function. Accept new solutions based on the change in the objective function and the current temperature. The cooling coefficient  $k$ , which approaches 1, controls the cooling rate and may vary over time. The annealing function is expressed as Equation (32). (iv) According to the Metropolis criterion in formula (33), if the new solution is better than the current one ( $E(x_{new}) < E(x_{old})$ , it is accepted; otherwise, it is accepted with a probability  $\exp((E(x_{old}) - E(x_{new}))/T)$ , allowing the search to escape local optima. (v) Gradually reduce the temperature until either the maximum number of iterations is reached or the termination temperature is met.

$$T_{n+1} = kT_n, k \in (0, 1) \quad (32)$$

$$p = \begin{cases} 1 & , E(x_{new}) < E(x_{old}) \\ \exp(-\frac{E(x_{new}) - E(x_{old})}{T}) & , E(x_{new}) \geq E(x_{old}) \end{cases} \quad (33)$$

Remarkably, SA is able to search in the neighborhood of the current solution, which is especially suitable for deep mining near the quality solutions already found. Through the Metropolis criterion, SA can effectively avoid falling into the local optimum and gradually converge to the global optimum. After the GA finds a better solution, SA can further optimize the details of the solution to improve the quality and feasibility of the solution.

#### (4) Solution evaluation and recording

(i) For each result of the local search optimization, the optimal solution and relevant information for each iteration are recorded to ensure tracking of performance improvements throughout the optimization process. (ii) The final iteration curve is plotted to illustrate the trend of the objective value changes during each iteration. The output includes the sequence numbers of the rail cars, the loading modes assigned to each container or EFC unit along with their layer numbers, and their respective positions within the layer. Additionally, the total transportation efficiency is calculated, considering the mixed grouping of well cars, shed cars, and tank cars.

**Algorithm 1** Hybrid Genetic Algorithm and Simulated Annealing Algorithm (Hybrid GA-SA) for the optimal loading of DSTs

```

Require: Input container data, General cargo and liquid bulk cargo data, rail car parameters, distances, and partial numerical constraints from the Excel file "Basic data.xlsx".
Ensure: (1) Assign containers with different O-Ds to well cars according to loading principles and determine their loading modes. (2) Accounts for mixed formations of well cars, shed cars, and tank cars, and finally calculate the total transport benefits.
Start
1: Step 1: Data Input and Initialization
2: Load data from the Excel file
3: Define 20 loading modes based on container characteristics (lengths, heights, loads, weights and shapes)
4: (1) Set the population size, maximum iterations for Hybrid GA-SA globally; (2) define the crossover probability, the mutation probability and the elite retention rate for GA section; (3) determine the initial temperature and the annealing coefficient for SA section.
5: Step 2: GA for Global Search
6: While termination condition not met do
7: Randomly generate an initial population (potential loading plan)
8: Evaluate fitness for each individual in population using fun 1
9: Based on the fitness values, use roulette wheel method to select the parent for generating individuals in the next generation
10: offspring ← []
11: for each pair of parents do
12: child ← Crossover(parents)
13: Append child to offspring
14: end for
15: for each child in offspring do
16: if random probability < mutation rate then
17: Mutate(child)
18: end if
19: end for
20: Elite ← Select the best individual from the population
21: population ← offspring + Elite
22:end while
23: Step 3: SA for Local Optimization
24: Current solution ← Use the best individual generated by GA as the initial solution for SA optimization
25: T ← initial temperature
26: while stopping condition not met do
27: New solution ← Generate new solutions within the neighborhood of the current solution and evaluate the fitness
28: ΔE ← E (new solution) – E (current solution)
29: if ΔE < 0 or random probability < exp(-ΔE/T) then
30: Current solution ← new solution
31: end if
32: Accept new solutions based on the Metropolis criterion
33: T ← k · T (k is the cooling coefficient) ▷ Cooling schedule
34: End while
35: Step 4: Solution Evaluation and Recording
36: Record best solution and related information
37: Plot the iteration curve of the best solution over iterations
38: Output final results (rail car number, loading mode, layer number and horizontal position for each container)
39: Compute the total transportation benefits considering the mixed grouping of well cars, shed cars, and tank cars.
End

```

## 5. Case experiment

### 5.1. Data preparation and model validity testing

To evaluate the effectiveness of the model, this study considers three terminal hubs (T) and three rail freight station hubs (S), with transport distances between them provided in [Table 5](#). The parameters required for the test case are summarized in [Table 6](#). The scenario includes 20 20-ft containers, 20 40-ft containers and EFC units, and 10 48-ft containers and EFC units, as shown in [Table 7](#). These containers are categorized by size (GC/HC) and type (loaded container, empty container, or EFC unit). Each container is transported from a designated hub T to hub S. Additionally, [Tables 7 and 9](#) detail 15 batches of general cargo and 10 batches of liquid bulk cargo, each with distinct origin and destination. Cargo/containers bound for earlier stops are placed at the rear of the train, while that for later stops are placed at the front. The experimental task is to assign containers with different origins and destinations to well cars according to loading principles ([Section 2.2](#)) and determine their loading modes (as shown in [Fig. 2](#)). During this process, each container is assigned to a specific position on the appropriate layer of the well car. The experiment also accounts for mixed formations of well cars, shed cars, and tank cars, ultimately calculating the total transport benefits.

In the hyperparameter tuning process, random search is used in this paper to determine the parameter combination that maximizes the performance of the model and the hybrid GA-SA. Compared to grid search, random search can randomly select hyperparameter combinations (larger search space) within a predefined domain of definition and search for consecutive values, so there is a chance to get better results. [Table 10](#) shows the tuning results of key parameters in the hybrid GA-SA.

### 5.2. Results discussion and methodological assessment

The model is run on a Windows 10 computer equipped with an Intel Core i5-10200H CPU (2.40 GHz) and 8.00 GB of RAM using Matlab 2021a programming. We use Matlab to call CPLEX for solving a small-scale case and find that it can load 50 containers and EFC units of various types and O-Ds onto 28 well cars in 41.257 s, calculating a total transportation benefit of 316,186 CNY. This demonstrates the model's effectiveness. To further evaluate its performance, we apply Hybrid GA-SA, SA, and GA to the same loading task, respectively. [Table 11](#) and [Fig. 9](#) present the average results of ten runs for each algorithm, along with the CPLEX solution. It is evident that Hybrid GA-SA outperforms both SA and GA in terms of iteration speed and computation time. CPLEX also produces a solution in a reasonable time, with a total benefit of 316,186 CNY. [Table 12](#) compares the solutions from each algorithm, including the well car arrangement and loading modes for each container and EFC unit. To accomplish this loading task, it is also found that CPLEX requires 27 well cars, GA uses 26, while both SA and Hybrid GA-SA only need 23 well cars.

When the task scale increases to 100 containers and EFC units, the performance of CPLEX shows a marked decline, taking 121.352 s to compute. In contrast, Hybrid GA-SA successfully finds the objective value of 534,494 CNY within 84.265 s, as illustrated in [Table 11](#) and [Fig. 10](#). At this point, CPLEX requires 54 well cars, GA uses 53 well cars, while both SA and Hybrid GA-SA only need 45 well cars. Due to the length of the loading scheme table for 100 containers and EFC units, the results are presented in Table A1 in Appendix A. The indices for all shed cars and tank cars are calculated in [Tables 8 and 9](#) based on the docking order for each batch of cargo. It is specified that shed cars and tank cars must be grouped consecutively and can only be positioned behind double-stack container well cars.

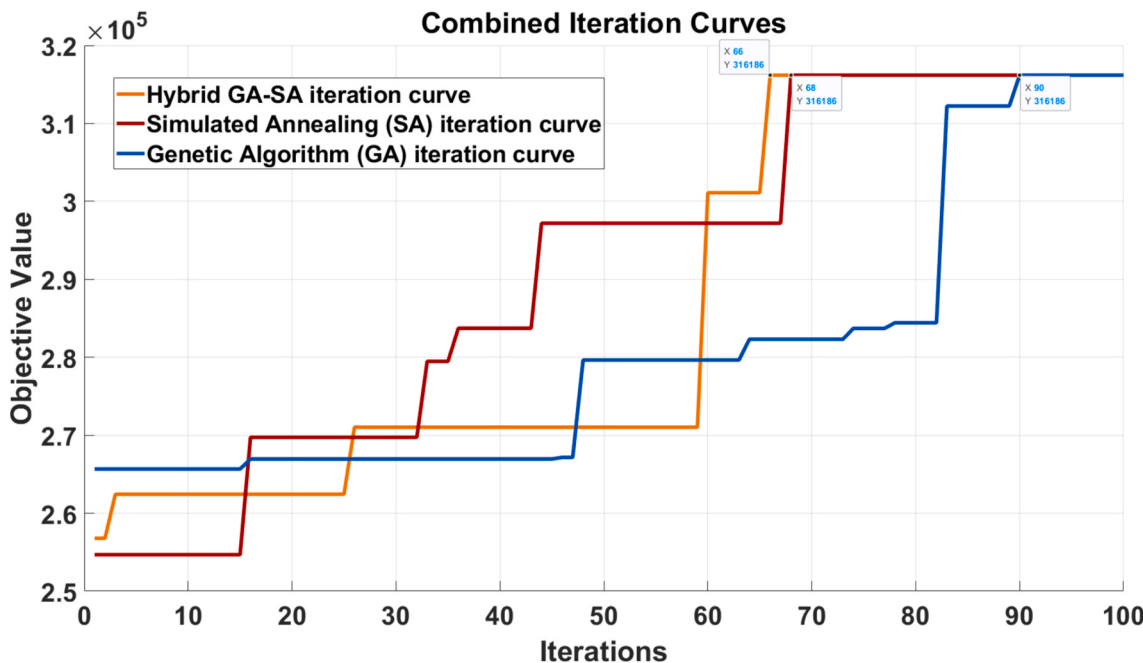


Fig. 9. Performance of three algorithms for solving 50 containers of different types and O-Ds.

### 5.3. Further exploration

Fig. 11 records the results for loading tasks of varying scales, with the input data for the 100-container scenario consistent with those in Section 4.2 and Appendix A. Each subsequent increase in mission size has been for these 100 containers and EFC units. It is obvious that the changes in the objective function value, the number of required well cars, and the computation time are not linear as the task size increases by 100 containers and EFC units. The objective function value experiences significant growth as the loading task scale goes from 100 to 200 containers (436,845 CNY); while the increase in total benefit from 200 to 400 containers is modest (331,917 CNY and 388,097 CNY, respectively). However, the growth in total benefit from 400 to 700 containers is substantial again (414,697 CNY and 428,696 CNY, respectively). The computation time demonstrates a threshold at a task size of 400 containers, initially showing a significant increase, which later tapers off. The number of well cars required for each loading task exhibits a similar pattern, though with smaller variations. This behavior indicates the reliability and superiority of the proposed model and the Hybrid GA-SA when addressing larger-scale scenarios.

This study compares the number of cars required for loading different scales of containers using DSTs versus conventional single-stack container trains (SSTs), as illustrated in Fig. 12. The former employs double-stack container well cars, while the latter uses single-stack container flat cars. For every set of 50 containers and EFC units (consistent with the data in Table 7 and Appendix A), the SST requires 40 flat cars. It is observed that as the scale of the loading task increases, the gap in the number of cars needed for the two types of trains widens. Additionally, assuming that the hourly usage and occupancy cost difference between the two types of rail cars is 30 CNY, the savings in car usage and occupancy costs also increase approximately linearly. This finding reflects that the loading plan developed in this study significantly contributes to reducing car costs and the consumption of capacity resources in large-scale loading tasks.

### 5.4. Sensitivity analysis

The experiment identifies six potential parameters that are most likely to affect transportation efficiency. Each parameter value is increased by 10 % to observe its impact on the objective function value, as shown in Fig. 13. Specifically, transportation efficiency is most sensitive to changes in the base freight rate 2 for the three types of goods, that is, a 10 % increase in item 2 results in an objective function value of 594,561 CNY, reflecting an increase of 11.24 %. In addition, an increase in transportation distance also significantly impacts transportation efficiency, leading to a 9.70 % rise in the objective function value. Besides, changes in the base freight rate for item 1, train speed, and the usage costs of the three types of rail cars have a smaller effect on transportation efficiency, with increases of 1.36 %, 2.15 %, and a decrease of 1.97 %, respectively. However, the variation in locomotive operating costs only has a negligible effect on the objective function value, resulting in a decrease of 0.62 %. This sensitivity analysis provides valuable decision-making support for railway operators in responding to market changes.

### 5.5. Investigation insights

In the investigation course, some pressing problems in the DST operation at Ningbo-Zhoushan Port are identified and referable management opinions are provided.

Firstly, the limited length and number of dedicated rail tracks and handling lines (handling platforms) for the DST not only affects the scheduling flexibility of the DST, but also restricts its connectivity with the national conventional rail system. For this reason, the government and industry are required to formulate a long-term development plan for DST operations, as well as introduce policies to support train upgrades and infrastructure development, including DST-standard railroad mileage and loading platform lengths.

Subsidiarily, the DST loading process requires additional manual intervention, such as installing the knob locks (corner pieces) at the corners of the lower containers, which significantly increases the

**Table 12**  
Loading solutions for 50 containers and EFC units.

Container data		CPLEX solution		SA solution		GA solution		Hybrid GA-SA solution	
Index	Type	Well car citation	Loading mode	Well car citation	Loading mode	Well car citation	Loading mode	Well car citation	Loading mode
1	20-ft LHC	2	16	4	1	2	16	4	1
2	20-ft LHC	2	16	4	1	2	16	4	1
3	20-ft LGC	1	4	7	1	1	4	5	1
4	20-ft LGC	3	17	7	1	3	17	5	1
5	20-ft LHC	4	17	8	1	4	17	9	16
6	20-ft LHC	5	17	8	1	5	17	9	16
7	20-ft LHC	1	4	18	3	1	4	19	3
8	20-ft LHC	6	16	18	3	7	3	19	3
9	20-ft LHC	6	16	9	16	7	3	8	1
10	20-ft LHC	8	16	9	16	10	1	8	1
11	20-ft EGC	8	16	5	14	10	1	11	19
12	20-ft EGC	9	19	5	14	8	19	11	19
13	20-ft EGC	9	19	12	14	8	19	12	14
14	20-ft EGC	7	10	12	14	6	10	12	14
15	20-ft EHC	10	4	11	19	9	17	7	14
16	20-ft EHC	11	17	11	19	10	1	7	14
17	20-ft EGC	7	10	13	14	6	10	13	14
18	20-ft EGC	10	4	13	14	7	3	13	14
19	20-ft EGC	13	16	14	14	11	16	14	14
20	20-ft EGC	13	16	14	14	11	16	14	14
1	40-ft LGC	12	20	16	17	12	20	16	17
2	40-ft LHC	14	19	1	4	13	19	1	4
3	40-ft LHC	14	19	2	17	13	19	2	17
4	40-ft LHC	15	14	3	17	15	14	3	17
5	40-ft LGC	15	14	4	1	15	14	4	1
6	40-ft LGC	16	14	6	4	16	14	5	1
7	40-ft LHC	16	14	7	1	16	14	6	4
8	40-ft LGC	18	19	19	4	17	19	18	4
9	40-ft LGC	18	19	8	1	17	19	8	1
10	40-ft LGC	15	14	17	4	14	20	17	4
11	40-ft EGC	16	14	12	14	15	14	12	14
12	40-ft EGC	17	20	5	14	16	14	7	14
13	40-ft EHC	19	11	13	14	18	11	13	14
14	40-ft EHC	19	11	14	14	18	11	14	14
15	40-ft EHC	20	4	10	20	19	17	10	20
16	40-ft EFC	21	17	15	11	20	4	15	11
unit									
17	40-ft EFC	20	4	20	11	20	4	20	11
18	40-ft EFC	23	3	21	11	22	3	21	11
19	40-ft EFC	23	3	22	11	22	3	22	11
20	40-ft EFC	22	4	23	11	21	4	23	11
unit									
1	48-ft LFC	22	4	17	4	21	4	1	4
2	48-ft LFC	23	3	1	4	22	3	6	4
3	48-ft LFC	24	11	18	3	23	11	17	4
4	48-ft LFC	25	11	19	4	24	11	18	4
5	48-ft LFC	26	11	6	4	25	11	19	3
6	48-ft EFC	27	11	15	11	26	11	15	11
unit									
7	48-ft EFC	24	11	20	11	23	11	20	11
8	48-ft EFC	25	11	21	11	24	11	21	11
9	48-ft EFC	26	11	22	11	25	11	22	11
10	48-ft EFC	27	11	23	11	26	11	23	11
unit									

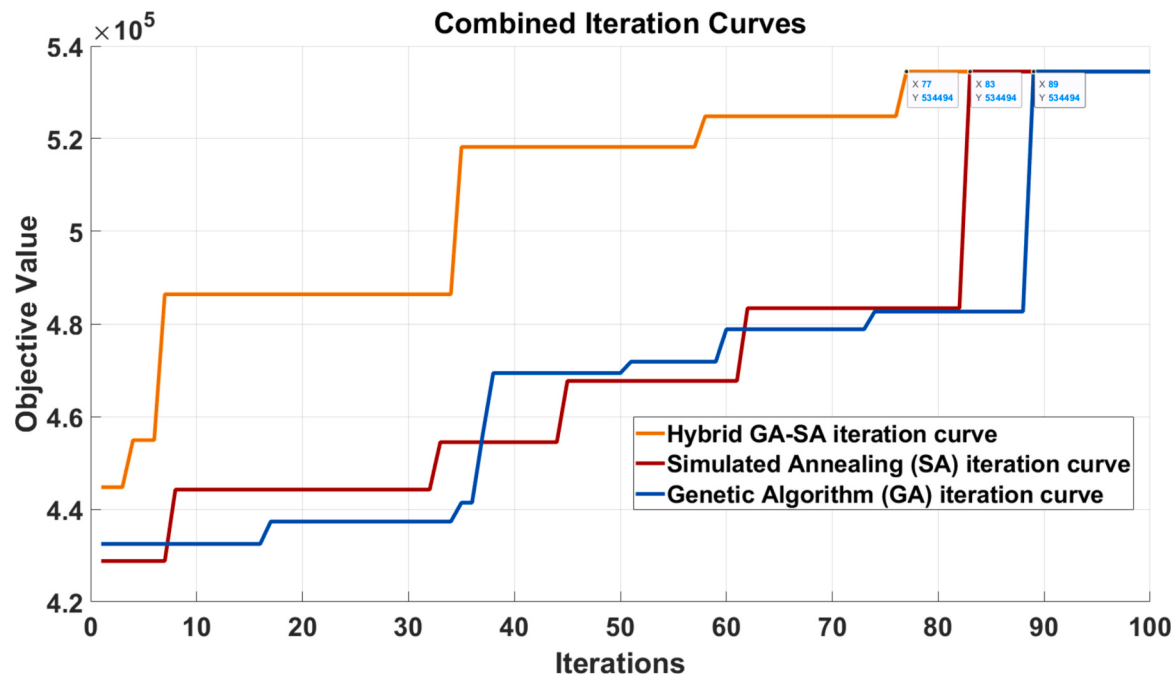


Fig. 10. Performance of three algorithms for solving 100 containers of different types and O-Ds.

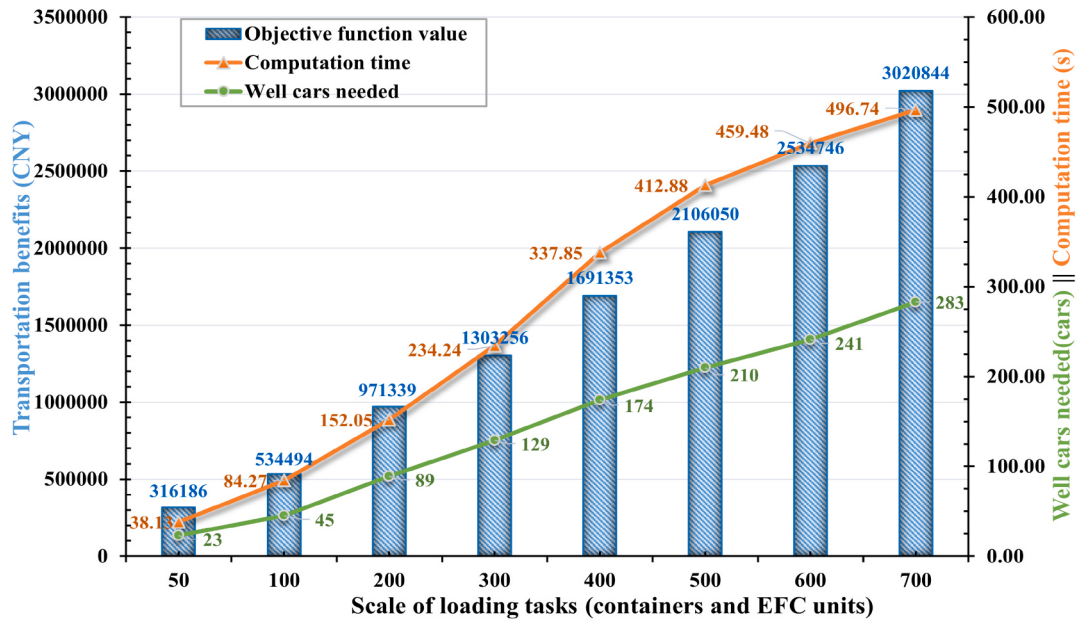


Fig. 11. Calculation results for different scales of loading tasks.

operating time. In the future, technologies such as automatic lock installation equipment and intelligent scheduling can be introduced into the handling operation to enhance operational efficiency and safety.

In addition, there is a limited number of well cars per DST (typically between 50 and 70), and such limitation may result from a combination of car design, railroad carrying capacity, and station scheduling capabilities. In light of this, research institutions need to optimize the design of DST locomotives and well cars, while exploring the technical feasibility of longer rail car groupings.

## 6. Conclusions

Optimizing the loading plan for electrified DSTs may help to enhance

transportation benefits and the handling capabilities at container terminals. This study contributes to the field through scenario analysis, mathematical modeling, algorithm improvement, and experimental analysis. The key contributions of this research are summarized as follows: (i) A detailed analysis of feasible and impractical loading modes for electrified DSTs in China is conducted, leading to the formulation of loading principles; (ii) A MIP model is developed to maximize the total benefits generated from transporting electrified DSTs across multiple hubs; (iii) The mixed loading of different types of containers and the mixed grouping of three types of rail cars are solved in the operation of DSTs. (iv) A hybrid GA-SA with optimal loading scheme is proposed and its reliability and superiority over hybrid GA-SA, GA, SA and CPLEX is demonstrated; (v) An analysis of different loading task scales reveals

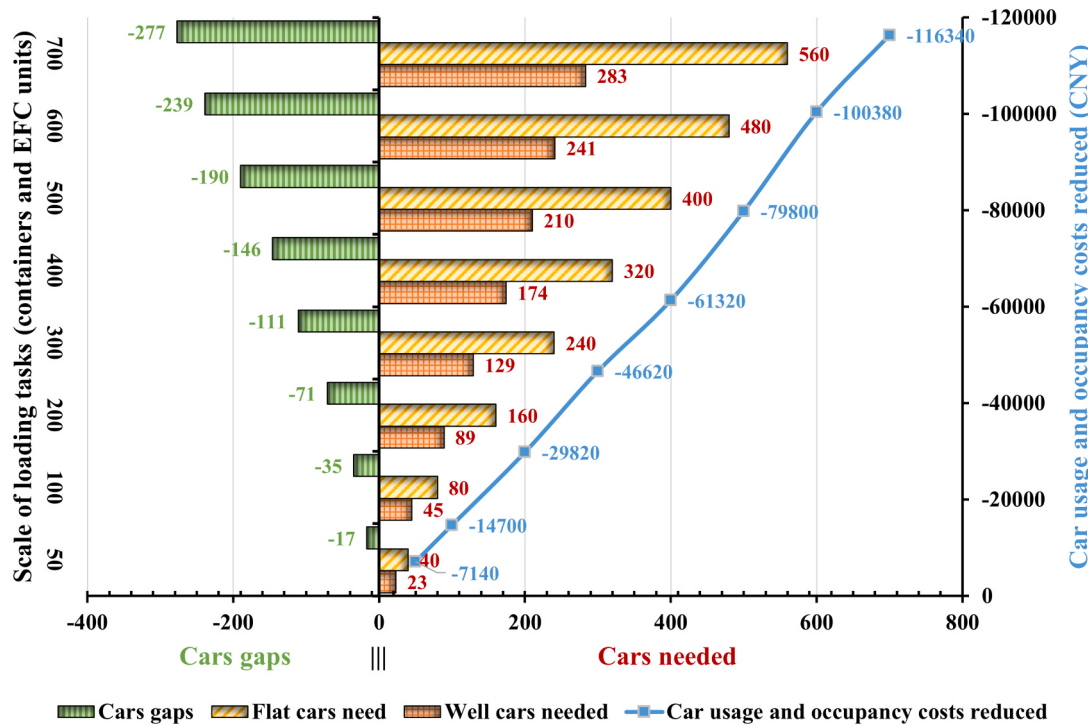


Fig. 12. Comparison of the number of cars required to load containers of different scales on double-stack container trains and conventional trains.

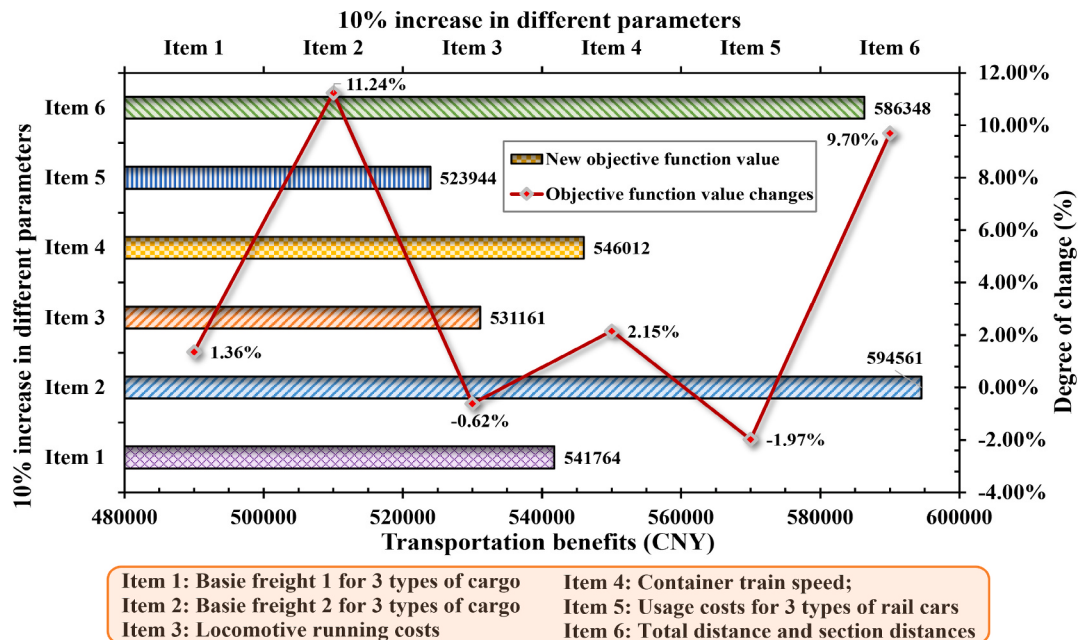


Fig. 13. Impact of a 10% increase in each of the six parameters on transport benefits.

that the proposed method can reduce well car costs and resource utilization in large-scale operations; (vi) The sensitivity analysis of six experimental parameters identifies the critical factors affecting total benefits.

However, this study primarily focuses on allocating containers to double-stack container well cars while also considering the mixed grouping of different types of rail cars. During the experiments on varying loading task scales, only the number of well cars is adjusted, without altering the configurations of shed cars and tank cars. Future research could explore the comprehensive impact of varying the quantities of all three types of rail cars on loading plans. Furthermore, the

model strictly adheres to China's electrified railway transportation constraints and the center of gravity limitations, which may necessitate the use of more well cars in the developed loading plans. It is recommended that railway management authorities consider revising current loading constraints and developing well cars with lower loading surfaces and center of gravity to achieve more optimal loading schemes.

#### CRediT authorship contribution statement

**Zhongbin Zhao:** Writing – original draft, Visualization, Validation, Software, Methodology, Investigation, Formal analysis, Data curation,

**Conceptualization.** **Jihong Chen:** Writing – review & editing, Writing – original draft, Supervision, Project administration, Funding acquisition, Data curation. **Mengru Shen:** Writing – review & editing, Resources, Methodology, Investigation. **Zheng Wan:** Writing – review & editing, Resources, Methodology, Formal analysis, Data curation. **Hao Wang:** Visualization, Validation, Software, Investigation. **Linlan Yu:** Data curation, Visualization, Writing – review & editing.

#### Declaration of competing interest

The authors declare that they have no known competing financial interests or personal relationships that could have appeared to influence

the work reported in this paper.

#### Acknowledgement

We would like to thank the editors and reviewers for their constructive comments, which tremendously improved the quality of this paper. In addition, this work is supported by the Natural Science Fundation of China (52472325) & Shen Zhen Key Research Base of Humanities and Social Sciences. We also appreciate the assistance and contributions from all the research team members of Shenzhen International Maritime Institute.

#### Appendix A . Loading solutions for 100 containers and EFC units

**Table A1**

Summary loading solutions for 100 containers and EFC units.

Container data		CPLEX solution		SA solution		GA solution		Hybrid GA-SA solution	
Index	Type	Well car citation	Loading mode	Well car citation	Loading mode	Well car citation	Loading mode	Well car citation	Loading mode
1	20-ft LHC	1	3	4	1	1	16	4	1
2	20-ft LHC	1	3	4	1	1	16	4	1
3	20-ft LGC	11	3	11	1	3	4	8	1
4	20-ft LGC	11	3	11	1	4	17	8	1
5	20-ft LHC	12	3	12	1	5	17	11	1
6	20-ft LHC	12	3	12	1	6	17	11	1
7	20-ft LHC	45	3	36	3	2	3	35	3
8	20-ft LHC	45	3	36	3	2	3	35	3
9	20-ft LHC	22	16	16	16	2	3	16	16
10	20-ft LHC	22	16	16	16	7	17	16	16
11	20-ft EGC	15	14	9	14	8	17	9	14
12	20-ft EGC	15	14	9	14	9	17	9	14
13	20-ft EGC	29	19	22	14	3	4	22	14
14	20-ft EGC	29	19	22	14	12	1	22	14
15	20-ft EHC	26	19	19	14	12	1	19	19
16	20-ft EHC	26	19	19	14	14	3	19	19
17	20-ft EGC	32	19	23	14	14	3	23	14
18	20-ft EGC	32	19	23	14	13	19	23	14
19	20-ft EGC	33	14	24	14	13	19	24	14
20	20-ft EGC	33	14	24	14	11	10	24	14
21	20-ft LHC	2	16	7	1	31	19	5	1
22	20-ft LHC	2	16	7	1	32	19	5	1
23	20-ft LGC	13	1	14	1	32	19	14	1
24	20-ft LGC	13	1	14	1	26	20	14	1
25	20-ft LHC	19	16	15	3	27	20	15	1
26	20-ft LHC	19	16	15	3	28	20	15	1
27	20-ft LHC	46	3	37	3	33	19	36	3
28	20-ft LHC	46	3	37	3	33	19	36	3
29	20-ft LHC	25	16	18	9	34	19	17	9
30	20-ft LHC	25	16	18	9	34	19	17	9
31	20-ft EGC	16	19	10	14	29	20	12	19
32	20-ft EGC	16	19	10	14	30	14	12	19
33	20-ft EGC	34	19	25	14	35	11	25	14
34	20-ft EGC	34	19	25	14	35	11	25	14
35	20-ft EHC	27	19	20	19	36	11	20	14
36	20-ft EHC	27	19	20	19	37	11	20	14
37	20-ft EGC	35	19	21	19	38	11	21	19
38	20-ft EGC	35	19	21	19	36	11	21	19
39	20-ft EGC	36	19	26	14	37	11	26	14
40	20-ft EGC	36	19	26	14	38	11	26	14
Container data		CPLEX solution		SA solution		GA solution		Hybrid GA-SA solution	
Index	Type	Well car citation	Loading mode	Well car citation	Loading mode	Well car citation	Loading mode	Well car citation	Loading mode
1	40-ft LGC	39	4	31	4	12	1	31	4
2	40-ft LHC	3	4	1	4	15	1	1	4

(continued on next page)

Table A1 (continued)

Container data		CPLEX solution		SA solution		GA solution		Hybrid GA-SA solution	
Index	Type	Well car citation	Loading mode	Well car citation	Loading mode	Well car citation	Loading mode	Well car citation	Loading mode
3	40-ft LHC	4	17	2	4	10	20	2	17
4	40-ft LHC	5	17	3	17	14	3	3	4
5	40-ft LGC	6	17	4	1	15	1	4	1
6	40-ft LGC	13	1	8	17	15	1	8	1
7	40-ft LHC	17	17	11	1	17	16	10	10
8	40-ft LGC	43	4	35	4	17	16	37	4
9	40-ft LGC	18	2	12	1	16	19	11	1
10	40-ft LGC	40	4	32	4	16	19	32	4
11	40-ft EGC	28	15	22	14	18	2	22	14
12	40-ft EGC	14	20	9	14	18	2	9	14
13	40-ft EHC	28	15	23	14	19	17	23	14
14	40-ft EHC	30	20	24	14	11	10	24	14
15	40-ft EHC	23	20	17	20	20	16	17	9
16	40-ft EFC	37	11	27	11	20	16	27	11
	unit								
17	40-ft EFC	47	11	40	11	21	20	40	11
	unit								
18	40-ft EFC	48	11	41	11	22	9	41	11
	unit								
19	40-ft EFC	49	11	42	11	22	9	42	11
	unit								
20	40-ft EFC	50	11	43	11	22	9	43	11
	unit								
21	40-ft LGC	41	17	33	17	39	4	33	4
22	40-ft LHC	7	17	34	4	40	17	34	17
23	40-ft LHC	8	17	5	17	39	4	5	1
24	40-ft LHC	9	17	6	17	41	4	6	17
25	40-ft LGC	10	17	7	1	42	4	7	17
26	40-ft LGC	18	2	13	2	41	4	13	4
27	40-ft LHC	20	17	13	2	42	4	14	1
28	40-ft LGC	44	4	14	1	43	3	15	1
29	40-ft LGC	21	17	38	17	43	3	38	4
30	40-ft LGC	42	17	39	4	45	17	39	17
31	40-ft EGC	31	15	19	14	43	3	20	14
32	40-ft EGC	15	14	10	14	44	3	10	10
33	40-ft EHC	31	15	25	14	44	3	25	14
34	40-ft EHC	33	14	26	14	44	3	26	14
35	40-ft EHC	24	20	18	9	46	4	18	20
36	40-ft EFC	38	11	28	11	47	4	28	11
	unit								
37	40-ft EFC	51	11	29	11	46	4	29	11
	unit								
38	40-ft EFC	52	11	44	11	47	4	44	11
	unit								
39	40-ft EFC	53	11	45	11	48	11	45	11
	unit								
40	40-ft EFC	54	11	30	11	49	11	30	11
	unit								
1	48-ft LFC	39	4	31	4	23	19	31	4
2	48-ft LFC	1	3	1	4	23	19	1	4
3	48-ft LFC	43	4	35	4	24	14	35	3
4	48-ft LFC	44	4	36	3	24	14	36	3
5	48-ft LFC	11	3	15	3	25	19	13	4
6	48-ft EFC	37	11	27	11	25	19	27	11
	unit								
7	48-ft EFC	47	11	40	11	24	14	40	11
	unit								
8	48-ft EFC	48	11	41	11	30	14	41	11
	unit								
9	48-ft EFC	49	11	42	11	30	14	42	11
	unit								
10	48-ft EFC	50	11	43	11	31	19	43	11
	unit								
11	48-ft LFC	40	4	32	4	50	11	32	4
12	48-ft LFC	3	4	34	4	51	11	33	4
13	48-ft LFC	45	3	2	4	48	11	3	4
14	48-ft LFC	46	3	37	3	49	11	37	4
15	48-ft LFC	12	3	39	4	50	11	38	4
16	48-ft EFC	38	11	28	11	51	11	28	11
	unit								
17	48-ft EFC	51	11	29	11	52	11	29	11

(continued on next page)

**Table A1 (continued)**

Container data		CPLEX solution		SA solution		GA solution		Hybrid GA-SA solution	
Index	Type	Well car citation	Loading mode	Well car citation	Loading mode	Well car citation	Loading mode	Well car citation	Loading mode
18	48-ft EFC unit	52	11	30	11	53	11	30	11
19	48-ft EFC unit	53	11	44	11	52	11	44	11
20	48-ft EFC unit	54	11	45	11	53	11	45	11

**Table A2**

Detailed Hybrid GA-SA solutions for 100 containers and EFC units.

1- No.	2- Container length	3-Empty container (0); Loaded container (1); EFC units (2)	4- Container weight	5- Container height	6-Base freight 1	7-Base freight 2	8- Origin	9- Destination	10- Classification of container length	11-Well car k number	12- Loading mode	13- Layer No. of the container belongs to	14- Horizontal No. of the container on this layer
1	20-ft	1	19.88	2896	440	3.185	1	1	1	4	1	1	1
2	20-ft	1	19.48	2896	440	3.185	1	1	1	4	1	1	2
3	20-ft	1	21.24	2591	440	3.185	1	2	1	8	1	1	1
4	20-ft	1	21.74	2591	440	3.185	1	2	1	8	1	1	2
5	20-ft	1	18.27	2896	440	3.185	1	2	1	11	1	1	1
6	20-ft	1	19.12	2896	440	3.185	1	2	1	11	1	1	2
7	20-ft	1	20.86	2896	440	3.185	3	2	1	35	3	1	1
8	20-ft	1	21.95	2896	440	3.185	3	2	1	35	3	1	2
9	20-ft	1	17.57	2896	440	3.185	1	3	1	16	16	1	1
10	20-ft	1	22.27	2896	440	3.185	1	3	1	16	16	1	2
11	20-ft	0	2.3	2591	440	3.185	1	2	1	9	14	1	1
12	20-ft	0	2.3	2591	440	3.185	1	2	1	9	14	1	2
13	20-ft	0	2.3	2591	440	3.185	2	2	1	22	14	1	1
14	20-ft	0	2.3	2591	440	3.185	2	2	1	22	14	1	2
15	20-ft	0	2.32	2896	440	3.185	2	1	1	19	19	1	1
16	20-ft	0	2.32	2896	440	3.185	2	1	1	19	19	1	2
17	20-ft	0	2.3	2591	440	3.185	2	2	1	23	14	1	1
18	20-ft	0	2.3	2591	440	3.185	2	2	1	23	14	1	2
19	20-ft	0	2.3	2591	440	3.185	2	2	1	24	14	1	1
20	20-ft	0	2.3	2591	440	3.185	2	2	1	24	14	1	2
21	20-ft	1	18.88	2591	440	3.185	1	1	1	5	1	1	1
22	20-ft	1	19.85	2591	440	3.185	1	1	1	5	1	1	2
23	20-ft	1	20.33	2591	440	3.185	1	2	1	14	1	1	1
24	20-ft	1	21.41	2591	440	3.185	1	2	1	14	1	1	2
25	20-ft	1	19.24	2591	440	3.185	1	2	1	15	1	1	1
26	20-ft	1	18.55	2591	440	3.185	1	2	1	15	1	1	2
27	20-ft	1	21.86	2896	440	3.185	3	2	1	36	3	1	1
28	20-ft	1	21.23	2896	440	3.185	3	2	1	36	3	1	2
29	20-ft	1	18.55	2591	440	3.185	1	3	1	17	9	1	1
30	20-ft	1	21.36	2591	440	3.185	1	3	1	17	9	1	2
31	20-ft	0	2.3	2591	440	3.185	1	2	1	12	19	1	1
32	20-ft	0	2.3	2591	440	3.185	1	2	1	12	19	1	2
33	20-ft	0	2.3	2591	440	3.185	2	2	1	25	14	1	1
34	20-ft	0	2.3	2591	440	3.185	2	2	1	25	14	1	2
35	20-ft	0	2.32	2896	440	3.185	2	1	1	20	14	1	1
36	20-ft	0	2.32	2896	440	3.185	2	1	1	20	14	1	2
37	20-ft	0	2.3	2591	440	3.185	2	1	1	21	19	1	1
38	20-ft	0	2.3	2591	440	3.185	2	1	1	21	19	1	2
39	20-ft	0	2.3	2591	440	3.185	2	2	1	26	14	1	1
40	20-ft	0	2.3	2591	440	3.185	2	2	1	26	14	1	2
41	40-ft	1	24.26	2591	532	3.357	3	1	2	31	4	1	1
42	40-ft	1	27.78	2896	532	3.357	1	1	2	1	4	1	1
43	40-ft	1	26.47	2896	532	3.357	1	1	2	2	17	1	1
44	40-ft	1	25.76	2896	532	3.357	1	1	2	3	4	1	1
45	40-ft	1	24.44	2591	532	3.357	1	1	2	4	1	2	1
46	40-ft	1	23.59	2591	532	3.357	1	2	2	8	1	2	1
47	40-ft	1	26.47	2896	532	3.357	1	2	2	10	10	1	1
48	40-ft	1	23.45	2591	532	3.357	3	2	2	37	4	1	1
49	40-ft	1	24.37	2591	532	3.357	1	2	2	11	1	2	1
50	40-ft	1	22.85	2591	532	3.357	3	1	2	32	4	1	1
51	40-ft	0	3.75	2591	532	3.357	2	2	2	22	14	2	1
52	40-ft	0	3.75	2591	532	3.357	1	2	2	9	14	2	1
53	40-ft	0	3.94	2896	532	3.357	2	2	2	23	14	2	1
54	40-ft	0	3.94	2896	532	3.357	2	2	2	24	14	2	1

(continued on next page)

Table A2 (continued)

1- No.	2- Container length	3-Empty container (0); Loaded container (1); EFC units (2)	4- Container weight	5- Container height	6-Base freight 1	7-Base freight 2	8- Origin	9- Destination	10- Classification of container length	11-Well car k number	12- Loading mode	13- Layer No. of the container belongs to	14- Horizontal No. of the container on this layer
55	40-ft	0	3.94	2896	532	3.357	1	3	2	17	9	2	1
56	40-ft	2	20	2591	532	3.357	2	3	2	27	11	1	1
57	40-ft	2	20	2591	532	3.357	3	3	2	40	11	1	1
58	40-ft	2	20	2591	532	3.357	3	3	2	41	11	1	1
59	40-ft	2	20	2591	532	3.357	3	3	2	42	11	1	1
60	40-ft	2	20	2591	532	3.357	3	3	2	43	11	1	1
61	40-ft	1	23.87	2591	532	3.357	3	1	2	33	4	1	1
62	40-ft	1	26.58	2896	532	3.357	3	1	2	34	17	1	1
63	40-ft	1	25.55	2896	532	3.357	1	1	2	5	1	2	1
64	40-ft	1	26.36	2896	532	3.357	1	1	2	6	17	1	1
65	40-ft	1	24.75	2896	532	3.357	1	1	2	7	17	1	1
66	40-ft	1	25.52	2591	532	3.357	1	2	2	13	4	1	1
67	40-ft	1	23.43	2896	532	3.357	1	2	2	14	1	2	1
68	40-ft	1	22.95	2896	532	3.357	1	2	2	15	1	2	1
69	40-ft	1	26.38	2896	532	3.357	3	2	2	38	4	1	1
70	40-ft	1	23.72	2591	532	3.357	3	2	2	39	17	1	1
71	40-ft	0	3.75	2591	532	3.357	2	1	2	20	14	2	1
72	40-ft	0	3.75	2591	532	3.357	1	2	2	10	10	2	1
73	40-ft	0	3.94	2896	532	3.357	2	2	2	25	14	2	1
74	40-ft	0	3.94	2896	532	3.357	2	2	2	26	14	2	1
75	40-ft	0	3.94	2896	532	3.357	1	3	2	18	20	1	1
76	40-ft	2	20	2591	532	3.357	2	3	2	28	11	1	1
77	40-ft	2	20	2591	532	3.357	2	3	2	29	11	1	1
78	40-ft	2	20	2591	532	3.357	3	3	2	44	11	1	1
79	40-ft	2	20	2591	532	3.357	3	3	2	45	11	1	1
80	40-ft	2	20	2591	532	3.357	2	3	2	30	11	1	1
81	48-ft	1	19.48	2591	650	3.516	3	1	3	31	4	2	1
82	48-ft	1	17.76	2591	650	3.516	1	1	3	1	4	2	1
83	48-ft	1	19.56	2591	650	3.516	3	2	3	35	3	2	1
84	48-ft	1	18.12	2591	650	3.516	3	2	3	36	3	2	1
85	48-ft	1	18.72	2591	650	3.516	1	2	3	13	4	2	1
86	48-ft	2	18	2591	650	3.516	2	3	3	27	11	2	1
87	48-ft	2	18	2591	650	3.516	3	3	3	40	11	2	1
88	48-ft	2	18	2591	650	3.516	3	3	3	41	11	2	1
89	48-ft	2	18	2591	650	3.516	3	3	3	42	11	2	1
90	48-ft	2	18	2591	650	3.516	3	3	3	43	11	2	1
91	48-ft	1	19.33	2591	650	3.516	3	1	3	32	4	2	1
92	48-ft	1	19.33	2591	650	3.516	3	1	3	33	4	2	1
93	48-ft	1	18.84	2591	650	3.516	1	1	3	3	4	2	1
94	48-ft	1	18.55	2591	650	3.516	3	2	3	37	4	2	1
95	48-ft	1	19.45	2591	650	3.516	3	2	3	38	4	2	1
96	48-ft	2	18	2591	650	3.516	2	3	3	28	11	2	1
97	48-ft	2	18	2591	650	3.516	2	3	3	29	11	2	1
98	48-ft	2	18	2591	650	3.516	2	3	3	30	11	2	1
99	48-ft	2	18	2591	650	3.516	3	3	3	44	11	2	1
100	48-ft	2	18	2591	650	3.516	3	3	3	45	11	2	1

## Data availability

The authors do not have permission to share data.

## References

- [1] A.S. Aghdam, A.T. Eshlaghy, M.A.A. Kazemi, A. Danehsvar, RFID network planning optimization using a genetic-simulated annealing combined algorithm, *China Commun.* 20 (8) (2023) 234–253, <https://doi.org/10.23919/JCC.fa.2021-0762.202308>.
- [2] W. Chen, J. Chen, J. Geng, J. Ye, T. Yan, J. Shi, J. Xu, Monitoring and evaluation of ship operation congestion status at container ports based on AIS data, *Ocean Coast. Manag.* 245 (2023) 106836, <https://doi.org/10.1016/j.ocemoaman.2023.106836>.
- [3] A. Gharehgozli, D. Roy, S. Saini, J.-K. van Ommeren, Loading and unloading trains at the landside of container terminals, *Maritime Econ. Logistics* 25 (3) (2023) 549–575, <https://doi.org/10.1057/s41278-022-00219-9>.
- [4] J. He, L. Zhang, Y. Deng, H. Yu, M. Huang, C. Tan, An allocation approach for external truck tasks appointment in automated container terminal, *Adv. Eng. Inf.* 55 (2023) 101864, <https://doi.org/10.1016/j.aei.2022.101864>.
- [5] H. Heggen, K. Braekers, A. Caris, A multi-objective approach for intermodal train load planning, *OR Spectr.* 40 (2) (2018) 341–366, <https://doi.org/10.1007/s00291-017-0503-1>.
- [6] Y. Jeong, G. Kim, Reliable design of container shipping network with foldable container facility disruption, *Transp. Res. Part E: Logistics Transport. Rev.* 169 (2023) 102964, <https://doi.org/10.1016/j.tre.2022.102964>.
- [7] E. Kurtulus, İ.B. Çetin, Analysis of modal shift potential towards intermodal transportation in short-distance inland container transport, *Transp. Policy* 89 (2020) 24–37, <https://doi.org/10.1016/j.tranpol.2020.01.017>.
- [8] L. Li, W. Du, X. Ma, J. Liu, H. Yuan, A model for investigating the coordination between low carbon and resilience performance in container terminals, *Ocean Coast. Manag.* 240 (2023) 106617, <https://doi.org/10.1016/j.ocemoaman.2023.106617>.
- [9] D.-Y. Lin, Y.-J. Kong, M. Ng, The double stack railcar allocation problem at marine container terminals, *J. Oper. Res. Soc.* (2023). <https://www.tandfonline.com/doi/abs/10.1080/01605682.2023.2294861>.
- [10] S. Mantovani, G. Morganti, N. Umang, T.G. Crainic, E. Freijinger, E. Larsen, The load planning problem for double-stack intermodal trains, *Eur. J. Oper. Res.* 267 (1) (2018) 107–119, <https://doi.org/10.1016/j.ejor.2017.11.016>.
- [11] H. Mokhtar, A.A.N.P. Redi, M. Krishnamoorthy, A.T. Ernst, An intermodal hub location problem for container distribution in Indonesia, *Comput. Oper. Res.* 104 (2019) 415–432, <https://doi.org/10.1016/j.cor.2018.08.012>.
- [12] M. Ng, W.K. Talley, Rail intermodal management at marine container terminals: loading double stack trains, *Transp. Res. Part C Emerging Technol.* 112 (2020) 252–259, <https://doi.org/10.1016/j.trc.2020.01.025>.
- [13] Y. Qu, Y. Kong, Z. Li, E. Zhu, Pursue the coordinated development of port-city economic construction and ecological environment: a case of the eight major ports

- in China, *Ocean Coast. Manag.* 242 (2023) 106694, <https://doi.org/10.1016/j.ocecoaman.2023.106694>.
- [14] P. Rathi, A. Upadhyay, Container retrieval and wagon assignment planning at container rail terminals, *Comput. Ind. Eng.* 172 (2022) 108626, <https://doi.org/10.1016/j.cie.2022.108626>.
- [15] M. Shen, Z. Zhao, H. Wang, X. Wang, Z. Jiang, K. Yang, Z. Wan, W. Liu, Round-trip multimodal transportation routes planning for foldable vehicle racks, *Marit. Policy Manag.* (2024). <https://www.tandfonline.com/doi/abs/10.1080/03088839.2024.2385847>.
- [16] S. Siri, A. Palmiere, D. Ambrosino, Multi-objective optimization methods for train load planning in seaport container terminals, *IEEE Trans. Automation Sci. Eng.* 1–13 (2023), <https://doi.org/10.1109/TASE.2023.3277083>.
- [17] J. Sun, R. Zhao, Analysis of environmental performance and interactivity of ports and regions, *Ocean Coast. Manag.* 239 (2023) 106602, <https://doi.org/10.1016/j.ocecoaman.2023.106602>.
- [18] W.K. Talley, M. Ng, Hinterland transport chains: a behavioral examination approach, *Transp. Res. Part E: Logistics Transp. Rev.* 113 (2018) 94–98, <https://doi.org/10.1016/j.tre.2018.03.001>.
- [19] Z. Tan, X. Zeng, T. Wang, Y. Wang, J. Chen, Capacity investment of shore power berths for a container port: environmental incentive and infrastructure subsidy policies, *Ocean Coast. Manag.* 239 (2023) 106582, <https://doi.org/10.1016/j.ocecoaman.2023.106582>.
- [20] D. Tang, Z. Chen, C. Xu, Y. Yuan, X. Zhong, C. Yuan, Energy consumption and emissions analysis of large container seaports considering the impact of COVID-19: a case study of Ningbo Zhoushan Port, *Ocean Coast. Manag.* 244 (2023) 106781, <https://doi.org/10.1016/j.ocecoaman.2023.106781>.
- [21] K. Tang, Y. Zhang, C. Yang, L. He, C. Zhang, W. Zhou, Optimization for multi-resource integrated scheduling in the automated container terminal with a parallel layout considering energy-saving, *Adv. Eng. Inf.* 62 (2024) 102660, <https://doi.org/10.1016/j.aei.2024.102660>.
- [22] Y. Tao, S. Zhang, C. Lin, X. Lai, A bi-objective optimization for integrated truck operation and storage allocation considering traffic congestion in container terminals, *Ocean Coast. Manag.* 232 (2023) 106417, <https://doi.org/10.1016/j.ocecoaman.2022.106417>.
- [23] A. Upadhyay, W. Gu, N. Bolia, Optimal loading of double-stack container trains, *Transp. Res. Part E: Logistics Transp. Rev.* 107 (2017) 1–22, <https://doi.org/10.1016/j.tre.2017.08.010>.
- [24] X. Xiang, C. Liu, L. Miao, Reactive strategy for discrete berth allocation and quay crane assignment problems under uncertainty, *Comput. Ind. Eng.* 126 (2018) 196–216, <https://doi.org/10.1016/j.cie.2018.09.033>.
- [25] B. Yan, J.G. Jin, X. Zhu, D.-H. Lee, L. Wang, H. Wang, Integrated planning of train schedule template and container transhipment operation in seaport railway terminals, *Transp. Res. Part E: Logistics Transp. Rev.* 142 (2020) 102061, <https://doi.org/10.1016/j.tre.2020.102061>.
- [26] B. Yan, X. Zhu, D.-H. Lee, J.G. Jin, L. Wang, Transhipment operations optimization of sea-rail intermodal container in seaport rail terminals, *Comput. Ind. Eng.* 141 (2020) 106296, <https://doi.org/10.1016/j.cie.2020.106296>.
- [27] C. Yin, Z. Zhang, X. Zhang, J. Chen, X. Tao, L. Yang, Hub seaport multimodal freight transport network design: perspective of regional integration development, *Ocean Coast. Manag.* 242 (2023) 106675, <https://doi.org/10.1016/j.ocecoaman.2023.106675>.
- [28] M. Yu, X. Liu, Z. Xu, L. He, W. Li, Y. Zhou, Automated rail-water intermodal transport container terminal handling equipment cooperative scheduling based on bidirectional hybrid flow-shop scheduling problem, *Comput. Ind. Eng.* 186 (2023) 109696, <https://doi.org/10.1016/j.cie.2023.109696>.
- [29] R. Zhang, C. Huang, X. Feng, Empty container repositioning with foldable containers in a river transport network considering the limitations of bridge heights, *Transp. Res. A Policy Pract.* 133 (2020) 197–213, <https://doi.org/10.1016/jтра.2020.01.019>.
- [30] S. Zhang, X. Ruan, Y. Xia, X. Feng, Foldable container in empty container repositioning in intermodal transportation network of Belt and Road Initiative: strengths and limitations, *Marit. Policy Manag.* 45 (3) (2018) 351–369, <https://doi.org/10.1080/03088839.2017.1400699>.
- [31] Z. Zhang, Z. Zhuang, W. Qin, R. Tan, C. Liu, H. Huang, Systems thinking and time-independent solutions for integrated scheduling in automated container terminals, *Adv. Eng. Inf.* 62 (2024) 102550, <https://doi.org/10.1016/j.aei.2024.102550>.
- [32] Z. Zhao, M. Shen, J. Chen, X. Wang, Z. Wan, X. Hu, W. Liu, Design and optimization of the collaborative container logistics system between a dry port and a water port, *Comput. Ind. Eng.* 198 (2024) 110654, <https://doi.org/10.1016/j.cie.2024.110654>.
- [33] Z. Zhao, X. Wang, S. Cheng, W. Liu, L. Jiang, A new synchronous handling technology of double stack container trains in sea-rail intermodal terminals, *Sustainability* 14 (18) (2022), <https://doi.org/10.3390/su141811254>. Article 18.